

# Accepted Manuscript

Synthesis of substituted phenanthrene-9-benzimidazole conjugates: Cytotoxicity evaluation and apoptosis inducing studies

Niggula Praveen Kumar, Pankaj Sharma, S. Sujana Kumari, Umarani Brahma, Shalini Nekkanti, Nagula Shankaraiah, Ahmed Kamal



PII: S0223-5234(17)30688-8

DOI: [10.1016/j.ejmech.2017.09.006](https://doi.org/10.1016/j.ejmech.2017.09.006)

Reference: EJMECH 9721

To appear in: *European Journal of Medicinal Chemistry*

Received Date: 21 June 2017

Revised Date: 21 August 2017

Accepted Date: 4 September 2017

Please cite this article as: N.P. Kumar, P. Sharma, S.S. Kumari, U. Brahma, S. Nekkanti, N. Shankaraiah, A. Kamal, Synthesis of substituted phenanthrene-9-benzimidazole conjugates: Cytotoxicity evaluation and apoptosis inducing studies, *European Journal of Medicinal Chemistry* (2017), doi: 10.1016/j.ejmech.2017.09.006.

This is a PDF file of an unedited manuscript that has been accepted for publication. As a service to our customers we are providing this early version of the manuscript. The manuscript will undergo copyediting, typesetting, and review of the resulting proof before it is published in its final form. Please note that during the production process errors may be discovered which could affect the content, and all legal disclaimers that apply to the journal pertain.

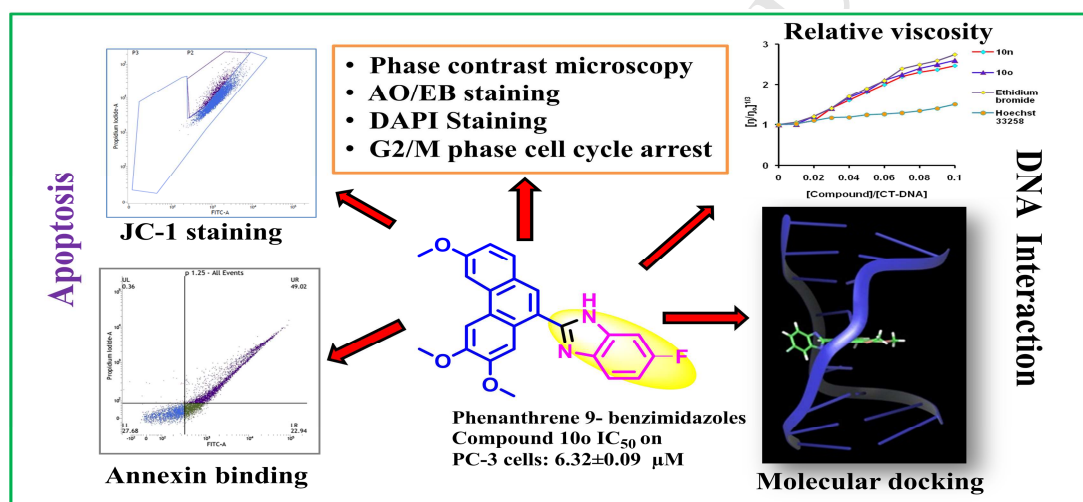
## Synthesis of substituted phenanthrene-9-benzimidazole conjugates: Cytotoxicity evaluation and apoptosis inducing studies

Niggula Praveen Kumar<sup>a</sup>, Pankaj Sharma<sup>a</sup>, S. Sujana Kumari<sup>b</sup>, Umarani Brahma<sup>b</sup>, Shalini Nekkanti<sup>a</sup>, Nagula Shankaraiah<sup>a,\*</sup>, Ahmed Kamal<sup>a,\*</sup>

<sup>a</sup>Department of Medicinal Chemistry, National Institute of Pharmaceutical Education and Research (NIPER), Hyderabad 500 037, India

<sup>b</sup>Department of Pharmacology and Toxicology, National Institute of Pharmaceutical Education and Research (NIPER), Hyderabad 500 037, India

### Graphical Abstract



## Synthesis of substituted phenanthrene-9-benzimidazole conjugates: Cytotoxicity evaluation and apoptosis inducing studies

Niggula Praveen Kumar<sup>a</sup>, Pankaj Sharma<sup>a</sup>, S. Sujana Kumari<sup>b</sup>, Umarani Brahma<sup>b</sup>, Shalini Nekkanti<sup>a</sup>, Nagula Shankaraiah<sup>a,\*</sup>, Ahmed Kamal<sup>a,\*</sup>

<sup>a</sup>*Department of Medicinal Chemistry, National Institute of Pharmaceutical Education and Research (NIPER), Hyderabad 500 037, India*

<sup>b</sup>*Department of Pharmacology and Toxicology, National Institute of Pharmaceutical Education and Research (NIPER), Hyderabad 500 037, India*

**Abstract:** A series of new phenanthrene-9-benzimidazole conjugates has been synthesized by condensing phenanthrene aldehydes with various substituted *o*-phenylenediamines. The title compounds were evaluated for their *in vitro* cytotoxic potential against various human cancer cell lines like breast (BT-549), prostate (PC-3 and DU145), triple negative breast cancer (MDA-MB-453), and human colon cancer (HCT-116 and HCT-15) cells. Among the tested compounds, **10o** displayed significant *in vitro* cytotoxic activity against PC-3 prostate cancer cells with an IC<sub>50</sub> value of 6.32±0.09 μM. Further, the cell cycle analysis indicated that it blocks G2/M phase of the cell cycle in a dose dependent manner. In order to determine the effect of the compound **10o** on cell viability; phase contrast microscopy, AO/EB staining, DAPI staining, and DCFDA staining studies were performed. In these studies, apoptotic features were clearly observed indicating that the compound inhibited cell proliferation by apoptosis. JC-1 staining and annexin binding assays indicated the extent of apoptosis in PC-3 cells. Further, relative viscosity measurements and molecular docking studies indicated that these compounds bind to DNA by intercalation.

**Keywords:** Benzimidazoles, phenanthrene, Perkin condensation, cytotoxicity, apoptosis, DNA interaction, molecular modeling.

\*Corresponding authors: Dr Ahmed Kamal, E-mail: [ahmedkamal@iict.res.in](mailto:ahmedkamal@iict.res.in); Dr Nagula Shankaraiah, E-mail: [shankar@niperhyd.ac.in](mailto:shankar@niperhyd.ac.in)

### 1. Introduction

Cancer is one of the lethal diseases worldwide and characterized by uncontrolled cell proliferation, metastasis and resistance to apoptotic signals [1]. Chemotherapeutic drugs that target the cell division, angiogenesis and apoptotic pathways are emerging as effective tools to combat cancer in the present drug discovery [2]. However, due to their off-target effects

and enhanced drug resistance in cancer cells, there is a demand to identify and synthesize novel efficacious and innocuous pharmacophores as chemotherapeutic agents [3]. DNA replication plays a crucial role in cancer cell division and planar cytotoxic agents such as doxorubicin, acridines, anthraquinones, distamycins, and phenanthrene derivatives are well known for targeting DNA [4]. In this context, the development of new molecular scaffolds that can act on DNA and induce apoptosis is of great importance [5]. Among the natural product derivatives, phenanthroindolizidine alkaloids from the *Asclepiadacea* [6] family represent a unique chemical class and are well established for their antitumor [7], antiangiogenic [8], antilupus [9], antiarthritis [10], antifungal [11], antimicrobial [12], and antiviral activities [13]. The most intriguing biological property among these alkaloids is their cytotoxic potential against various cancer cell lines [14]. This is due to the intercalation of the phenanthrene core between the DNA base pairs [15] and also inhibition of the enzymes involved in DNA synthesis [16]. Tylophorine (**Figure 1**) is one of the representative alkaloids of this class.

On the other hand, benzimidazole, a nitrogen containing heterocyclic is regarded as the “Master Key” as it is the vital pharmacophore in numerous bioactive agents targeting various proteins [17]. *N*-Ribosyl-dimethyl benzimidazole exists naturally and serves as an axial ligand for cobalt in vitamin B<sub>12</sub> [18]. Benzimidazoles are structural isosteres of nucleobases owing to their fused nitrogen nuclei [19]. They are capable of interacting with biomolecular targets and exhibit numerous activities such as antiproliferative [20], anti-inflammatory [21], antiallergic [22], antibacterial [23] and antiviral [24] properties. Furthermore, recent studies revealed that some of the naturally existing and synthetic benzimidazoles are potent anticancer agents and their activity is due to their interaction with the DNA double helix [25]. Abonia *et al* reported the quinolinone-benzimidazoles (**Figure 1**) as potential antitumour agents [26]. A few benzimidazoles tethered to planar naphthalimide rings were also established as drug leads [27]. Telmisartan possessing an *N*-benzylated benzimidazole core is reported to induce early apoptosis in the prostate cancer cells [28]. Moreover, in medicinal chemistry, functionalization of the known active scaffolds based on SAR to access diverse bioactive molecules is of high rationale.

The earlier reports reveal that the presence of polar moieties at C9-position of the planar phenanthrene skeleton is of great importance for their cytotoxic activity [29]. Tethering of polar benzimidazole nucleus at the C9-position might effectively enhance the antitumor activity. In continuation of our research dedicated to bioactive scaffolds [30],

herein we have designed and synthesized a series of new phenanthrene-9-benzimidazole conjugates. The newly synthesized compounds **10a–q** were further evaluated for their *in vitro* cytotoxicity, and cell growth inhibition studies.

<Insert Figure 1 here>

## 2. Results and discussion

### 2.1 Chemistry

The synthetic strategy for the preparation of phenanthrene-9-benzimidazole conjugates **10a–q** was depicted in **Scheme 1**. Various substituted *o*-phenylenediamines **9a–l** were condensed with phenanthrene-9-carbaldehydes (**5a,b**). The aldehyde partners **5a** and **5b** were synthesized from the commercially available starting materials *via* the conventional five step sequence [31]. Initially, Perkin condensation of the substituted benzaldehydes **2a,b** and 3,4-dimethoxy phenyl acetic acid **1** resulted in the formation of substituted diphenyl acrylic acids. Next, the acid was converted into its methyl ester **3** followed by *m*-CPBA/TFA mediated intramolecular oxidative cyclization to give the tricyclic phenanthrene esters **4a,b**. However, in case of R = H this reaction was carried in the presence of FeCl<sub>3</sub> and *m*-CPBA. Further, the ester functionality was reduced to alcohol by LiAlH<sub>4</sub>. The alcohols were oxidized by using Dess-Martin periodinane reagent to give the respective phenanthrene-9-carbaldehydes **5a,b**. For the synthesis of *N*-substituted *o*-phenylenediamines, 4-chloro-2-nitro aniline was initially benzylated using benzyl bromides and later the nitro group was reduced to amino functionality by stannous chloride dihydrate as shown in **Scheme 2**. Finally, the title compounds **10a–q** were synthesized by refluxing phenanthrene-9-carbaldehydes and *o*-phenylenediamines in ethanol in the presence of sodium metabisulphite. All the newly synthesized compounds **10a–q** were characterized by HRMS, <sup>1</sup>H and <sup>13</sup>C NMR spectroscopy.

<Insert Scheme 1 here>

<Insert Scheme 2 here>

### 2.2 Pharmacology

#### 2.2.1 Cytotoxic activity

The newly synthesized phenanthrene-9-benzimidazole conjugates **10a–q** were screened for their *in vitro* cytotoxicity on different human cancer cell lines such as breast (BT-549), prostate (PC-3 and DU145), triple negative breast cancer (MDA-MB-453), and human colon cancer (HCT-116 and HCT-15) by using 3-(4,5-dimethylthiazol-2-yl)-2,5-

diphenyltetrazolium bromide (MTT) assay [32]. The  $IC_{50}$  ( $\mu M$ ) values (concentration required to inhibit 50% of the tumor cells) of the tested compounds and the positive controls, 5-fluorouracil and nocodazole are listed in **Table 1**. It is noticeable from the preliminary screening that a majority of the tested compounds displayed cytotoxicity less than 20  $\mu M$  on the PC-3 prostate cancer cell line. The compound **10o** with a fluoro substitution on benzimidazole nucleus was found to show the highest potency on PC-3 cell line ( $IC_{50}$   $6.32 \pm 0.09 \mu M$ ). **10d**, **10e**, **10g**, **10k**, and **10l** displayed cytotoxic activities against a majority of the cancer cell lines with  $IC_{50}$  values ranging from  $8.34 \pm 0.15 \mu M$  to  $17.3 \pm 0.31 \mu M$  (**Table 2**). It was observed that, only the derivatives **10e**, **10g** and **10n** were active against the HCT-116 colon cancer cells with  $IC_{50}$  values of  $9.92 \pm 0.82$ ,  $8.91 \pm 0.72$  and  $11.3 \pm 0.46 \mu M$  respectively. Compounds **10b**, **10c**, **10e**, **10g**, **10k**, **10l**, **10o**, and **10p** displayed  $IC_{50}$  values less than 20  $\mu M$  in the MDA-MB-453 breast cancer cells, among which, the compound **10o** possessing fluoro group as  $R^3$  substituent proved to be best with an  $IC_{50}$  of  $6.61 \pm 0.9 \mu M$ . This is followed by the compound **10p** with a benzyl substituted nitrogen atom and a chloro substitution on benzimidazole aromatic ring displayed  $IC_{50}$   $7.20 \pm 0.18 \mu M$  and then compound **10c**, a chloro benzimidazole having a free *NH* ( $IC_{50}$   $9.42 \pm 0.14 \mu M$ ). Derivatives **10d** and **10q** showed activity less than 10  $\mu M$  on the BT-549 breast cancer cell line with **10q** ( $R^3 = Br$ ,  $X = N$ ) being the most active ( $IC_{50}$   $7.91 \pm 0.23 \mu M$ ) followed by **10d** ( $R^3 = F$ ,  $IC_{50}$   $10.8 \pm 0.06 \mu M$ ). Interestingly, the compound **10g** with a methoxy benzimidazole substitution at the C9-position was found to be active on all the cell lines except DU-145 with the most potent activity ( $IC_{50}$   $8.91 \pm 0.72 \mu M$ ) on HCT-116 colon cancer cell line. The derivatives **10d**, **10e**, **10g**, **10k**, **10l**, and **10p** displayed cytotoxicity against HCT-15 colon cancer cells with  $IC_{50}$  values ranging from  $8.34 \pm 0.15 \mu M$  to  $15.6 \pm 0.16 \mu M$ . Compound **10f** with  $R^3 = COOCH_3$  substitution proved to be moderately active against the PC-3 and DU-145 prostate cancer cell lines with  $IC_{50}$  values of  $16.7 \pm 0.72 \mu M$  and  $17.2 \pm 0.42 \mu M$ , respectively. It could be easily observed from the *in vitro* cytotoxicity data that these new derivatives with electro negative substituents like fluoro and chloro benzimidazoles at the C9-position of phenanthrene scaffold augmented the biological response. The electronegative nucleus of these groups connected to carbon atom with-draws electrons from other parts of the molecule, thus strongly polarizing the bond and may enhance interaction with biomolecular targets [33]. Based on the encouraging results, one of the most active compounds **10o** was taken-up for further examining the mechanism of cancer cell growth inhibition and DNA viscosity study.

<Insert Table 1 here>

### 2.2.2 Morphology studies using microscopy

Microscopic examination was performed to know whether the treatment with these compounds could lead to reduced cancer cell viability [34]. PC-3 prostate cancer cells were treated with 2.5, 5.0 and 10.0  $\mu\text{M}$  concentrations of the active compound **10o**. Cells were observed and the images were captured by a phase contrast microscope. It is clearly observed from **Figure 2** that the increased concentration of the compound **10o** led to the decreased number of viable cells in comparison to control, as observed by significant morphological changes such as nuclear shrinkage and cell detachment. This indicates that the compounds induced distinctive morphological changes on PC-3 cells.

*<Insert Figure 2 here>*

### 2.2.3 Acridine orange-ethidium bromide (AO-EB) staining

Acridine orange/ethidium bromide (AO/EB) fluorescent staining assay was performed to differentiate between live cells, necrotic and apoptotic cells [35]. AO readily diffuses through the intact cell membrane and stains the nuclei green, whereas EB enters only the membrane disintegrated cells and stains the nucleus red. **Figure 3** shows green colour in case of control cells due to their normal morphology. Fluorescence microscopic images of cells treated with 10.0  $\mu\text{M}$  of the compound **10o** clearly showed the altered morphological characteristics such as chromatin condensation, apoptotic body formation, cell shrinkage and membrane blebbing suggesting that the compound **10o** induced cell death on PC-3 cells.

*<Insert Figure 3 here>*

### 2.2.4 DAPI staining

DAPI (4',6-diamidino-2-phenylindole) is a fluorescent stain that reveals the chromatin condensation or nuclear damage through effectively binding to A-T rich regions of DNA. DAPI permeates the intact cell membrane with less efficiency when compare to damaged cell membrane. Therefore, the intensity of staining in live cells is less whereas apoptotic cells are stained bright due to the presence of condensed nucleus which is a typical apoptotic characteristic. Therefore, it is considered of our interest to examine the effect of the compound **10o** on PC-3 cells by using DAPI staining [36]. This technique is useful to distinguish live cells from apoptotic cells based on their nuclear morphology. DAPI forms fluorescent complex with chromatin there by stains the nucleus bright blue. As observed from **Figure 4**, the nuclear structure of control cells was intact, whereas compound **10o** treated PC-3 cells exhibited apoptotic features such as horse-shoe shaped and condensed nuclei.

<Insert Figure 4 here>

### 2.2.5 Cell cycle analysis

Many of the cytotoxic agents display their growth inhibitory potential by arresting the cell cycle at a specific point. Thus, the blockade of cell cycle progression by cytotoxic compounds has an important role in the action of a potential chemotherapeutic agent. From *in vitro* screening, it is apparent that the compound **10o** displayed significant anticancer activity against PC-3 prostate cancer cells. Therefore, we studied the effect of compound **10o** on distribution of the cell population in different phases of cell cycle by flow cytometry analysis [37]. PC-3 cells were treated with compound **10o** at 2.5  $\mu$ M, 5.0  $\mu$ M and 10.0  $\mu$ M for 24 h, and the cells were fixed by ethanol, stained with propidium iodide and further analyzed by flow cytometry. The results from **Figure 5** shows that the ratio of PC-3 cells in G2/M phase from 25.9% in control increased to 27.8% at 2.5  $\mu$ M, 29.7% at 5.0  $\mu$ M and 44.1% at 10.0  $\mu$ M respectively and simultaneous decreased number of cell population in G0/G1 phase. Therefore, these result clearly indicated that compound **10o** arrests G2/M phase of cell cycle in PC-3 cells.

<Insert Figure 5 here>

### 2.2.6 Measurement of reactive oxygen species (ROS)

The production of ROS is a typical characteristic of many cytotoxic agents by initiating oxidative damage to the mitochondrial membrane potential and permeability. Hence, DCFDA staining method [38] has been used to assess the generation of intracellular ROS on PC-3 cells by the compound **10o**. PC-3 cells were treated with compound **10o** at 2.5  $\mu$ M, 5.0  $\mu$ M and 10.0  $\mu$ M for 6 h, which resulted in enhanced DCFDA fluorescence in a dose dependent manner, indicating the accumulation of ROS (**Figure 6**). On the other hand, decreased fluorescence intensity was observed when PC-3 cells were treated with *N*-acetyl cysteine (NAC) prior to the compound treatment. This indicated the decreased free radical production by NAC, thereby suggesting that the compounds induced cytotoxicity by ROS generation. Moreover, H<sub>2</sub>O<sub>2</sub> treatment of PC-3 cells led to the increased fluorescence when compared to the control due to the generation of radicals.

<Insert Figure 6 here>

### 2.2.7 Analysis of mitochondrial membrane potential ( $D\Psi_m$ )

Enhanced ROS generation can cause oxidative stress there by leading to altered mitochondrial membrane potential. Therefore, JC-1 staining was performed to study the

effect of the compound **10o** on mitochondrial membrane potential ( $D\Psi_m$ ). The lipophilic cationic JC-1 dye was used to stain the mitochondria [39]. Normal polarised mitochondria stains red due to the formation of J-aggregates, whereas the depolarised mitochondria of apoptotic cells stains green because of J-monomers. PC-3 cells were treated with 2.5, 5.0 and 10.0  $\mu\text{M}$  of compound **10o** for 24 h and stained with JC-1 dye. Flow-cyometric analysis of the treated cells clearly displayed an increase in depolarised cell population (P3) from 22.8 of control to 33.35, 67.42 and 95.64, respectively in a concentration dependent manner (**Figure 7**). Thus, the results indicate loss of mitochondrial membrane potential ( $D\Psi_m$ ) by the compound **10o**.

*<Insert Figure 7 here>*

### 2.2.8 AnnexinV-FITC/Propidium iodide dual staining assay

Annexin V-FITC/propidium iodide dual staining assay [40] was performed to determine the extent of apoptosis induced by the compound **10o** on PC-3 cells. This assay facilitates the detection of necrotic cells (Q1-UL; AV-/PI+), live cells (Q1-LL; AV-/PI-), early apoptotic cells (Q1-LR; AV+/PI-), and late apoptotic cells (Q1- UR; AV+/PI+). As observed from **Figure 8**, the percentage of total apoptotic cells (early and late apoptotic cells) increased to 71.96% after treatment with 10  $\mu\text{M}$  concentration of **10o** for 24 h, in comparison to the control (22.68%) cells. The percentage of early and late apoptotic cells comparatively increased with an increase in the concentration of compound **10o**, which indicates the induction of dose dependent apoptosis in PC-3 cancer cells.

*<Insert Figure 8 here>*

### 2.2.9 Relative viscosity experiment

Relative viscosity experiments provide the evidence for the mode of interaction of the most potent compounds **10n** and **10o** with DNA [41]. Intercalation of molecules sandwiched between the DNA base pairs results in a major enhancement in the viscosity of DNA solutions; but a minor alteration in viscosity is shown by groove binders or DNA surface binders. Interestingly, covalent DNA-binders reduce the relative viscosity of DNA solutions. At this juncture, we have used Ethidium Bromide, Doxorubicin and Hoechst 33258 as controls. Ethidium bromide and Doxorubicin, the intercalators increased the relative viscosity strongly by lengthening the DNA strands; while relative viscosity increased only a little in case of Hoechst 33258, a minor groove binder. On gradually increasing the concentration of the compounds **10n** and **10o**, there was a noticeable increase in the relative viscosity of the

complex solutions, which suggests DNA intercalation of these derivatives. Upon interaction with DNA, **10o** produced an increase in viscosity comparable to that of Ethidium bromide and Doxorubicin, indicating strong DNA binding affinity (**Figure 9**). The data obtained from viscosity studies are consistent with the results obtained from the *in vitro* cytotoxicity studies.

<Insert Figure 9 here>

### 2.2.10 Molecular docking

Molecular docking simulations were performed into the DNA duplex d(GAAGCTTC)<sub>2</sub> using XP Glide 6.9 (Schrödinger 2015-4). The docked poses for the top scored compounds **10n** and **10o**, shown in **Figure 10**, depict comfortable insertion of the phenanthrene ring between the G–C base pairs. Interestingly, the benzimidazole ring lies at right angles to the planar phenanthrene ring system due to steric effects and orients itself perfectly in the minor groove. The docked poses were stabilized electronically by  $\pi$ – $\pi$  stacking, dipole-dipole interactions and formation of hydrogen-bonds between the *NH*-hydrogen of benzimidazole and the DNA base pairs. The results obtained from molecular docking studies were consistent with the *in vitro* cytotoxicity as well as relative viscosity data.

<Insert Figure 10 here>

## 3. Conclusion

In conclusion, a new series of C9-tethered phenanthrene benzimidazoles were synthesized and these compounds were evaluated for their *in vitro* cytotoxic potential against various human cancer cell lines. From the initial screening, it was observed that some of the derivatives were active on most of the tested cancer cell lines with IC<sub>50</sub> values below 20  $\mu$ M. The cytotoxicity profile indicated that the most active compound **10o** showed broad range of activity on three of the tested cell lines with a remarkable IC<sub>50</sub> value of  $6.32 \pm 0.09$   $\mu$ M on PC-3 prostate cancer cells. The compound **10o** blocked the cell cycle progression at G2/M phase in a dose dependent manner. Moreover, the compound also led to a decrease in the number of viable cells and increased apoptotic features as shown in case of phase contrast microscopy, AO/EB and DAPI staining. JC-1 staining and annexin binding assays indicated the dose-dependent apoptosis by compound **10o** on PC-3 cells. Further, increasing the concentrations of compounds **10n** and **10o** lead to increased viscosity suggesting that these compounds binds to DNA by intercalation. Molecular docking study also supports the DNA interaction of these new compounds. Overall, the current study established that these

phenanthren-9-benzimidazole conjugates have the potential to be advanced as DNA interactive cytotoxic agents for the treatment of prostate cancer.

## 4. Experimental protocols

### 4.1 Chemistry

All reagents and solvents were obtained from commercial suppliers and were used without further purification. Analytical thin layer chromatography (TLC) was performed on MERCK precoated silica gel 60-F<sub>254</sub> (0.5 mm) aluminum plates. Visualization of the spots on TLC plates was achieved by UV light. <sup>1</sup>H and <sup>13</sup>C NMR spectra were recorded on Bruker 500 MHz making a solution of samples in CDCl<sub>3</sub> and DMSO-*d*<sub>6</sub> solvent using tetramethyl silane (TMS) as the internal standard. Chemical shifts for <sup>1</sup>H and <sup>13</sup>C are reported in parts per million (ppm) downfield from tetra methyl silane. Spin multiplicities are described as s (singlet), bs (broad singlet), d (doublet), dd (double doublet), t (triplet), q (quartet), and m (multiplet). Coupling constant (*J*) values are reported in hertz (Hz). HRMS were determined with Agilent QTOF mass spectrometer 6540 series instrument. Wherever required, column chromatography was performed using silica gel 60-120 or 100-200) or neutral alumina. The reactions wherever anhydrous conditions required are carried under nitrogen positive pressure using freshly distilled solvents. All evaporation of solvents was carried out under reduced pressure on rotary evaporator below 45 °C.

#### 4.1.1 2,3,6,7-tetramethoxyphenanthrene-9-carbaldehyde (**5a**).

Yellow solid, yield 76%; mp: 183–184 °C; <sup>1</sup>H NMR (500 MHz, CDCl<sub>3</sub>): δ 10.24 (s, 1H), 8.94 (s, 1H), 8.02 (s, 1H), 7.75 (s, 1H), 7.73 (s, 1H), 7.30 (s, 1H), 4.15 (s, 3H), 4.12 (s, 3H), 4.09 (s, 3H), 4.05 (s, 3H) ppm; <sup>13</sup>C NMR (125 MHz, CDCl<sub>3</sub>): δ 193.8, 152.0, 150.0, 149.3, 149.0, 139.1, 127.9, 127.8, 124.9, 124.5, 122.9, 109.3, 106.1, 102.5, 102.4, 56.0, 55.9, 55.9, 55.8 ppm; HRMS (ESI): *m/z* calcd for C<sub>19</sub>H<sub>18</sub>O<sub>5</sub> 327.1227, found 327.1210 [M + H]<sup>+</sup>.

#### 4.1.2 3,6,7-trimethoxyphenanthrene-9-carbaldehyde (**5b**).

Colourless solid, yield 71%; mp: 169–171°C; <sup>1</sup>H NMR (500 MHz, CDCl<sub>3</sub>): δ 10.19 (s, 1H), 8.92 (s, 1H), 8.01 (s, 1H), 7.89 (d, *J* = 8.69 Hz, 1H), 7.78 (s, 1H), 7.75 (s, 1H), 7.23-7.21 (m, 1H), 4.08 (d, *J* = 1.67 Hz, 6H), 4.03 (s, 3H) ppm; <sup>13</sup>C NMR (125 MHz, CDCl<sub>3</sub>): δ 193.8, 161.0, 150.5, 149.2, 140.3, 134.1, 132.1, 127.4, 124.7, 124.2, 123.8, 116.0, 106.2, 103.9, 103.0, 55.9, 55.8, 55.5 ppm; HRMS (ESI): *m/z* calcd for C<sub>18</sub>H<sub>16</sub>O<sub>4</sub> 297.1121, found 297.1115 [M + H]<sup>+</sup>.

#### 4.1.3 General reaction procedure for benzylation of 4-chloro-2-nitro aniline **8a–b**

The mixture of 4-chloro-2-nitroaniline **6** (1.0 mmol) and benzyl bromides **7a**, **7b** (1.2 mmol) in water (4 mL) was refluxed at 100°C for 2h. After completion of the reaction as monitored by TLC, the reaction mixture was cooled and extracted with ethylacetate. The organic layer was dried over sodium sulphate and concentrated under vacuum. The obtained crude solid was further purified by column chromatography by using ethyl acetate/n-hexane to afford the pure compounds **8a–b**. All the synthesized compounds were characterized by <sup>1</sup>H NMR and <sup>13</sup>C NMR spectroscopy.

##### 4.1.3.1 *N*-benzyl-4-chloro-2-nitroaniline (**8a**).

Red solid, yield 83%; mp: 78–80 °C; <sup>1</sup>H NMR (500 MHz, DMSO-*d*<sub>6</sub>): δ 8.73 (t, *J* = 6.10 Hz, 1H), 8.06 (d, *J* = 2.59 Hz, 1H), 7.49-7.47 (m, 1H), 7.35-7.31 (m, 4H), 7.26-7.23 (m, 1H), 6.94 (d, *J* = 9.30 Hz, 1H), 4.64 (d, *J* = 6.25 Hz, 2H) ppm; <sup>13</sup>C NMR (125 MHz, DMSO-*d*<sub>6</sub>): δ 143.6, 138.0, 136.0, 131.1, 128.5, 127.0, 126.7, 124.8, 118.4, 116.9, 45.6 ppm.

##### 4.1.3.2 4-chloro-*N*-(3,5-dimethylbenzyl)-2-nitroaniline (**8b**).

brown liquid, yield 80%; <sup>1</sup>H NMR (500 MHz, DMSO-*d*<sub>6</sub>): δ 8.67 (t, *J* = 5.95 Hz, 1H), 8.04 (d, *J* = 2.59 Hz, 1H), 7.48-7.46 (m, 1H), 6.93 (s, 2H), 6.91 (d, *J* = 9.30 Hz, 1H), 6.86 (s, 1H), 4.53 (d, *J* = 6.10 Hz, 2H), 2.21 (s, 6H) ppm; <sup>13</sup>C NMR (125 MHz, DMSO-*d*<sub>6</sub>): δ 143.7, 137.9, 137.5, 136.0, 131.0, 128.5, 124.8, 124.4, 118.4, 116.9, 45.7, 20.8 ppm.

#### 4.1.4 General reaction procedure for Substituted *O*-phenylene diamines **9k–l**

To a mixture of benzyl nitro anilines **8a**, **8b** (1.0 mmol) in ethanol was added stannous chloride dihydrate (4.0 mmol) and the reaction was stirred at room temperature for 12 h. After completion of the reaction as monitored by TLC, sodium bicarbonate solution was added and extracted with ethyl acetate. The organic layer was dried over sodium sulphate and concentrated under vacuum. The obtained crude solid was further purified by column chromatography by using ethyl acetate/n-hexane to afford the pure compounds **9k–l**. All the synthesized compounds were characterized by <sup>1</sup>H NMR and <sup>13</sup>C NMR spectroscopy.

##### 4.1.4.1 *N*<sup>1</sup>-benzyl-4-chlorobenzene-1,2-diamine (**9k**).

Orange liquid, yield 70%; <sup>1</sup>H NMR (500 MHz, DMSO-*d*<sub>6</sub>): δ 7.35-7.29 (m, 4H), 7.23-7.17 (m, 1H), 6.56 (d, *J* = 2.44 Hz, 1H), 6.38-6.36 (m, 1H), 6.27 (d, *J* = 8.39 Hz, 1H), 5.23 (t, *J* = 5.79 Hz, 1H), 4.91 (s, 2H), 4.28 (d, *J* = 5.79 Hz, 2H) ppm; <sup>13</sup>C NMR (125 MHz, DMSO-*d*<sub>6</sub>): δ 139.8, 136.9, 134.1, 128.1, 127.0, 126.5, 120.3, 115.9, 112.8, 110.8, 46.7 ppm.

#### 4.1.4.2 4-chloro-*N*<sup>1</sup>-(3,5-dimethylbenzyl)benzene-1,2-diamine (**9l**).

Yellow liquid, yield 68%; <sup>1</sup>H NMR (500 MHz, DMSO-*d*<sub>6</sub>): δ 6.95 (s, 2H), 6.84 (s, 1H), 6.60 (s, 1H), 6.41 (d, *J* = 8.39 Hz, 1H), 6.28 (d, *J* = 8.39 Hz, 1H), 5.15 (t, *J* = 5.79 Hz, 1H), 4.90 (s, 2H), 2.23 (s, 6H) ppm; <sup>13</sup>C NMR (125 MHz, DMSO-*d*<sub>6</sub>): δ 139.8, 137.1, 136.9, 134.4, 128.1, 124.8, 120.3, 116.1, 113.0, 110.8, 46.9, 20.9 ppm.

#### 4.1.5 General reaction procedure for the synthesis of compounds **10a–q**

To an aqueous solution of Na<sub>2</sub>S<sub>2</sub>O<sub>5</sub> (1.5 mmol), was added the corresponding *o*-phenylene diamine (**9a–l**) (1.0 mmol) followed by a solution of phenanthrene aldehydes **5a,b** (1.0 mmol) in ethanol and the reaction mixture was stirred at 70 °C. After completion of the reaction, the reaction mixture was cooled; water was added and left to stand for 1 h at 0 °C to obtain the precipitate. The obtained crude solid was filtered and further purified by column chromatography by using ethyl acetate/*n*-hexane to afford the pure compounds **10a–q**. All the synthesized compounds were characterized by HRMS (ESI), <sup>1</sup>H NMR and <sup>13</sup>C NMR spectroscopy.

##### 4.1.5.1 2-(2,3,6,7-Tetramethoxyphenanthren-9-yl)-1*H*-benzo[*d*]imidazole (**10a**).

Off white solid, yield 85%; mp: 210–212 °C; <sup>1</sup>H NMR (500 MHz, DMSO-*d*<sub>6</sub>): δ 12.92 (s, 1H), 8.80 (s, 1H), 8.17 (s, 1H), 8.11 (s, 1H), 8.07 (s, 1H), 7.77 (d, *J* = 7.62 Hz, 1H), 7.58 (d, *J* = 7.47 Hz, 1H), 7.47 (s, 1H), 7.28–7.22 (m, 2H), 4.08 (s, 6H), 3.94 (s, 3H), 3.87 (s, 3H) ppm; <sup>13</sup>C NMR (125 MHz, DMSO-*d*<sub>6</sub>): δ 152.0, 150.1, 149.0, 148.8, 148.5, 143.8, 134.2, 126.3, 124.9, 124.8, 124.7, 123.3, 123.2, 122.4, 121.3, 118.9, 111.1, 108.6, 107.5, 103.8, 103.5, 55.9, 55.8, 55.4, 55.1 ppm; HRMS (ESI): *m/z* calcd for C<sub>25</sub>H<sub>22</sub>N<sub>2</sub>O<sub>4</sub> 415.1652, found 415.1665 [M + H]<sup>+</sup>.

##### 4.1.5.2 6-Bromo-2-(2,3,6,7-tetramethoxyphenanthren-9-yl)-1*H*-benzo[*d*]imidazole (**10b**).

White solid, yield 82%; mp: 157–159 °C; <sup>1</sup>H NMR (500 MHz, DMSO-*d*<sub>6</sub>): δ 13.14 (d, *J* = 18.9 Hz, 1H), 8.74 (s, 1H), 8.18 (s, 1H), 8.11 (s, 1H), 8.07 (s, 1H), 7.55 (d, *J* = 8.54 Hz, 1H), 7.73 (d, *J* = 8.39 Hz, 1H), 7.48 (d, *J* = 2.74 Hz, 1H), 7.41–7.36 (m, 1H), 4.08 (d, *J* = 2.44 Hz, 6H), 3.94 (s, 3H), 3.87 (s, 3H) ppm; <sup>13</sup>C NMR (125 MHz, DMSO-*d*<sub>6</sub>): δ 153.4, 150.2, 149.1, 148.8, 148.6, 145.2, 133.4, 126.6, 124.9, 124.8, 124.7, 123.0, 122.6, 121.2, 120.6, 113.6, 112.9, 108.7, 107.3, 103.8, 103.5, 55.9, 55.8, 55.4, 55.1 ppm; HRMS (ESI): *m/z* calcd for C<sub>25</sub>H<sub>21</sub>BrN<sub>2</sub>O<sub>4</sub> 493.0957, found 493.0766 [M + H]<sup>+</sup>.

##### 4.1.5.3 6-Chloro-2-(2,3,6,7-tetramethoxyphenanthren-9-yl)-1*H*-benzo[*d*]imidazole (**10c**).

Off white solid, yield 77%; mp: 225–227 °C; <sup>1</sup>H NMR (300 MHz, CDCl<sub>3</sub> + DMSO-*d*<sub>6</sub>): δ 8.25 (s, 1H), 7.86 (s, 1H), 7.72–7.65 (m, 4H), 7.28–7.25 (m, 1H), 7.10 (s, 1H), 4.13 (s, 3H), 4.11 (s, 3H), 3.99 (s, 3H), 3.91 (s, 3H) ppm; <sup>13</sup>C NMR (125 MHz, CDCl<sub>3</sub>+ DMSO-*d*<sub>6</sub>): δ 153.2, 149.6, 148.5, 148.3, 148.2, 126.9, 126.4, 124.6, 124.5, 124.3, 123.1, 122.8, 122.0, 121.1, 115.4, 114.4, 113.6, 107.9, 106.6, 102.2, 102.0, 55.5, 55.4, 55.3, 55.1 ppm; HRMS (ESI): *m/z* calcd for C<sub>25</sub>H<sub>21</sub>ClN<sub>2</sub>O<sub>4</sub> 449.1263, found 449.1261 [M + H]<sup>+</sup>.

#### 4.1.5.4 6-Fluoro-2-(2,3,6,7-tetramethoxyphenanthren-9-yl)-1H-benzo[d]imidazole (**10d**).

Light brown solid, yield 76%; mp: 229–231 °C; <sup>1</sup>H NMR (300 MHz, DMSO-*d*<sub>6</sub>): δ 8.53 (s, 1H), 7.98 (s, 1H), 7.85 (d, *J* = 11.51 Hz, 2H), 7.75 (s, 1H), 7.31–7.22 (m, 2H), 6.95 (t, *J* = 9.61 Hz, 1H), 4.07 (s, 6H), 3.94 (s, 3H), 3.90 (s, 3H) ppm; <sup>13</sup>C NMR (125 MHz, DMSO-*d*<sub>6</sub> + CDCl<sub>3</sub>): δ 158.0, 153.6, 150.4, 149.3, 149.1, 148.8, 126.7, 125.2, 125.1, 123.4, 123.1, 110.4, 110.2, 108.9, 107.4, 103.7, 103.4, 56.1, 56.0, 55.8, 55.5 ppm; HRMS (ESI): *m/z* calcd for C<sub>25</sub>H<sub>21</sub>FN<sub>2</sub>O<sub>4</sub> 433.1558, found 433.1571 [M + H]<sup>+</sup>.

#### 4.1.5.5 2-(2,3,6,7-Tetramethoxyphenanthren-9-yl)-1H-benzo[d]imidazole-6-carboxylic acid (**10e**).

Brown solid, yield 62%; mp: 240–242 °C; <sup>1</sup>H NMR (500 MHz, DMSO-*d*<sub>6</sub>): δ 13.25 (s, 1H), 8.83–8.74 (m, 1H), 8.36–8.17 (m, 2H), 8.12 (s, 1H), 8.08 (s, 1H), 7.96–7.63 (m, 2H), 7.50 (d, *J* = 11.29 Hz, 1H), 4.08 (s, 6H), 3.94 (s, 3H), 3.89 (s, 3H) ppm; <sup>13</sup>C NMR (125 MHz, DMSO-*d*<sub>6</sub>): δ 167.9, 153.9, 150.3, 149.1, 148.9, 148.6, 137.5, 126.8, 125.0, 124.9, 124.7, 124.2, 123.9, 123.0, 122.8, 122.5, 120.7, 110.9, 108.7, 107.3, 103.8, 103.5, 55.9, 55.8, 55.4, 55.1 ppm; HRMS (ESI): *m/z* calcd for C<sub>26</sub>H<sub>22</sub>N<sub>2</sub>O<sub>6</sub> 459.1551, found 459.1552 [M + H]<sup>+</sup>.

#### 4.1.5.6 Methyl 2-(2,3,6,7-tetramethoxyphenanthren-9-yl)-1H-benzo[d]imidazole-6-carboxylate (**10f**).

Brown solid, yield 60%; mp: 165–167 °C; <sup>1</sup>H NMR (500 MHz, DMSO-*d*<sub>6</sub>): δ 8.78 (s, 1H), 8.29–8.22 (m, 2H), 8.12 (s, 1H), 8.08 (s, 1H), 7.92 (d, *J* = 8.39 Hz, 1H), 7.76–7.74 (m, 1H), 7.49 (s, 1H), 4.09 (s, 6H), 3.94 (s, 3H), 3.90 (d, *J* = 4.73 Hz, 6H), ppm; <sup>13</sup>C NMR (125 MHz, DMSO-*d*<sub>6</sub>): δ 166.7, 154.6, 150.3, 149.1, 148.9, 148.6, 131.7, 126.8, 125.0, 124.8, 124.7, 123.2, 123.0, 122.3, 108.7, 107.2, 106.5, 105.4, 103.8, 103.5, 55.9, 55.8, 55.4, 55.1, 51.9 ppm; HRMS (ESI): *m/z* calcd for C<sub>27</sub>H<sub>24</sub>N<sub>2</sub>O<sub>6</sub> 473.1707, found 473.1715 [M + H]<sup>+</sup>.

#### 4.1.5.7 6-Methoxy-2-(2,3,6,7-tetramethoxyphenanthren-9-yl)-1H-benzo[d]imidazole (**10g**).

Brown solid, yield 78%; mp: 219–211 °C; <sup>1</sup>H NMR (500 MHz, DMSO-*d*<sub>6</sub>): δ 12.78 (s, 1H),

8.81 (s, 1H), 8.13 (s, 1H), 8.10 (s, 1H), 8.06 (s, 1H), 7.65-7.45 (m, 2H), 7.27-7.01 (m, 1H), 6.88 (d,  $J = 8.54$  Hz, 1H), 4.07 (s, 6H), 3.93 (s, 3H), 3.87 (s, 3H), 3.83 (s, 3H) ppm;  $^{13}\text{C}$  NMR (125 MHz,  $\text{DMSO-}d_6$ ):  $\delta$  150.0, 149.0, 148.8, 148.5, 126.0, 124.8, 124.6, 123.3, 123.2, 108.6, 107.6, 103.8, 103.5, 55.9, 55.8, 55.5, 55.4, 55.2 ppm; HRMS (ESI):  $m/z$  calcd for  $\text{C}_{26}\text{H}_{24}\text{N}_2\text{O}_5$  445.1758, found 445.1774  $[\text{M} + \text{H}]^+$ .

4.1.5.8 6-Methyl-2-(2,3,6,7-tetramethoxyphenanthren-9-yl)-1H-benzo[d]imidazole (**10h**).

white solid, yield 80%; mp: 221–223 °C;  $^1\text{H}$  NMR (500 MHz,  $\text{DMSO-}d_6$ ):  $\delta$  8.75 (s, 1H), 8.14 (s, 1H), 8.10 (s, 1H), 8.06 (s, 1H), 7.56 (d,  $J = 8.08$  Hz, 1H), 7.47-7.45 (m, 2H), 7.09-7.08 (m, 1H), 4.07 (s, 6H), 3.93(s, 3H), 3.87(s, 3H), 2.46(s, 3H) ppm;  $^{13}\text{C}$  NMR (125 MHz,  $\text{CDCl}_3+\text{DMSO-}d_6$ ):  $\delta$  151.6, 149.6, 148.6, 148.4, 148.3, 131.5, 126.2, 124.7, 124.4, 123.5, 123.4, 123.3, 114.1, 108.1, 106.9, 102.4, 102.2, 55.6, 55.5, 55.4, 55.1, 21.2 ppm; HRMS (ESI):  $m/z$  calcd for  $\text{C}_{26}\text{H}_{24}\text{N}_2\text{O}_4$  429.1809, found 429.1822  $[\text{M} + \text{H}]^+$ .

4.1.5.9 5,7-Dimethyl-2-(2,3,6,7-tetramethoxyphenanthren-9-yl)-1H-benzo[d]imidazole (**10i**).

Off white solid, yield 83%; mp: 268–270 °C;  $^1\text{H}$  NMR (500 MHz,  $\text{DMSO-}d_6$ ):  $\delta$  12.71 (s, 1H) 9.17-8.81 (m, 1H), 8.19 (s, 1H), 8.10 (s, 1H), 8.07 (s, 1H), 7.47 (s, 1H), 7.25-7.22 (m, 1H), 6.87 (s, 1H), 4.08 (s, 6H), 3.94 (s, 3H), 3.89 (s, 3H), 2.58 (s, 3H), 2.42 (s, 3H) ppm;  $^{13}\text{C}$  NMR (125 MHz,  $\text{DMSO-}d_6$ ):  $\delta$  151.0, 150.0, 148.9, 148.8, 148.4, 131.2, 127.4, 126.0, 125.9, 124.8, 124.6, 124.2, 123.6, 123.3, 123.1, 108.6, 107.7, 105.2, 103.7, 103.5, 55.9, 55.7, 55.4, 54.9, 21.2, 16.5 ppm; HRMS (ESI):  $m/z$  calcd for  $\text{C}_{27}\text{H}_{26}\text{N}_2\text{O}_4$  443.1965, found 443.1975  $[\text{M} + \text{H}]^+$ .

4.1.5.10 6-Bromo-2-(2,3,6,7-tetramethoxyphenanthren-9-yl)-1H-imidazo[4,5-b]pyridine (**10j**).

Brown solid, yield 71%; mp: 211–213 °C;  $^1\text{H}$  NMR (300 MHz,  $\text{DMSO-}d_6$ ):  $\delta$  10.24 (s, 1H), 8.93 (s, 1H), 8.08 (s, 1H), 7.81 (d,  $J = 7.74$  Hz, 2H), 7.50-7.36 (m, 2H), 4.16 (d,  $J = 9.25$  Hz, 6H), 4.07 (d,  $J = 6.04$  Hz, 6H), ppm;  $^{13}\text{C}$  NMR (125 MHz,  $\text{DMSO-}d_6 + \text{CDCl}_3$ ):  $\delta$  159.3, 155.1, 149.3, 148.9, 143.8, 131.6, 130.7, 127.9, 124.6, 124.2, 124.0, 121.5, 116.4, 112.7, 107.3, 104.0, 103.8, 55.7, 55.6, 55.4, 55.2 ppm; HRMS (ESI):  $m/z$  calcd for  $\text{C}_{24}\text{H}_{20}\text{BrN}_3\text{O}_4$  494.0710, found 494.0713  $[\text{M} + \text{H}]^+$ .

4.1.5.11 1-Benzyl-5-chloro-2-(2,3,6,7-tetramethoxyphenanthren-9-yl)-1H-benzo[d]imidazole (**10k**).

Off white solid, yield 81%; mp: 234–236 °C;  $^1\text{H}$  NMR (500 MHz,  $\text{CDCl}_3$ ):  $\delta$  7.90 (d,  $J =$

1.22 Hz, 1H), 7.86 (s, 1H), 7.83 (s, 1H), 7.63 (s, 1H), 7.28-7.24 (m, 2H), 7.22-7.18 (m, 3H), 7.15 (s, 1H), 7.08 (s, 1H), 6.94-6.92 (m, 2H), 5.26 (s, 2H), 4.15 (d,  $J = 6.86$  Hz, 6H), 4.00 (s, 3H), 3.77 (s, 3H) ppm;  $^{13}\text{C}$  NMR (125 MHz,  $\text{CDCl}_3$ ):  $\delta$  154.6, 150.3, 149.5, 149.1, 149.1, 144.0, 135.7, 133.7, 128.7, 128.1, 127.8, 127.5, 126.5, 125.4, 125.0, 124.9, 124.8, 123.4, 123.0, 119.8, 111.4, 108.5, 106.0, 102.9, 102.6, 56.1, 56.0, 55.9, 55.7, 48.5 ppm; HRMS (ESI):  $m/z$  calcd for  $\text{C}_{32}\text{H}_{27}\text{ClN}_2\text{O}_4$  539.1732, found 539.1762  $[\text{M} + \text{H}]^+$ .

4.1.5.12 *5-Chloro-1-(3,5-dimethylbenzyl)-2-(2,3,6,7-tetramethoxyphenanthren-9-yl)-1H-benzo[d]imidazole (10l)*.

White solid, yield 79%; mp: 175–177 °C;  $^1\text{H}$  NMR (500 MHz,  $\text{CDCl}_3$ ):  $\delta$  7.89-7.78 (m, 3H), 7.62 (s, 1H), 7.34-7.27 (m, 2H), 7.10 (s, 2H), 6.81 (s, 1H), 6.49 (s, 2H), 5.16 (s, 2H), 4.16 (s, 3H), 4.14 (s, 3H), 4.00 (s, 3H), 3.75 (s, 3H), 2.11 (s, 6H) ppm;  $^{13}\text{C}$  NMR (125 MHz,  $\text{CDCl}_3$ ):  $\delta$  154.5, 150.2, 149.4, 149.0, 144.0, 139.2, 138.2, 135.5, 133.8, 129.4, 127.9, 127.4, 125.3, 125.0, 124.8, 123.3, 123.3, 119.7, 111.4, 109.3, 108.5, 106.0, 102.8, 102.5, 56.0, 55.9, 55.8, 55.6, 48.4, 21.1 ppm; HRMS (ESI):  $m/z$  calcd for  $\text{C}_{34}\text{H}_{31}\text{ClN}_2\text{O}_4$  567.2045, found 567.2036  $[\text{M} + \text{H}]^+$ .

4.1.5.13 *2-(3,6,7-Trimethoxyphenanthren-9-yl)-1H-benzo[d]imidazole (10m)*.

White solid, yield 80%; mp: 247–249 °C;  $^1\text{H}$  NMR (300 MHz,  $\text{DMSO}-d_6$ ):  $\delta$  8.53 (s, 1H) 8.02 (s, 1H), 7.89 (s, 1H), 7.82 (d,  $J = 5.66$  Hz, 1H), 7.77-7.73 (m, 2H), 7.54 (s, 1H), 7.31-7.27 (m, 2H), 7.22-7.19 (m, 1H), 4.13 (s, 3H), 4.05 (s, 3H), 3.95 (s, 3H) ppm;  $^{13}\text{C}$  NMR (125 MHz,  $\text{CDCl}_3 + \text{DMSO}-d_6$ ):  $\delta$  159.0, 151.9, 149.3, 148.9, 131.3, 130.6, 126.9, 124.6, 124.5, 124.4, 122.7, 121.9, 116.5, 107.6, 104.2, 104.0, 55.8, 55.5, 55.2 ppm; HRMS (ESI):  $m/z$  calcd for  $\text{C}_{24}\text{H}_{20}\text{N}_2\text{O}_3$  385.1547, found 385.1548  $[\text{M} + \text{H}]^+$ .

4.1.5.14 *6-Chloro-2-(3,6,7-trimethoxyphenanthren-9-yl)-1H-benzo[d]imidazole (10n)*.

White solid, yield 82%; mp: 213–215 °C;  $^1\text{H}$  NMR (500 MHz,  $\text{DMSO}-d_6$ ):  $\delta$  8.81 (d,  $J = 4.42$  Hz, 1H), 8.22 (s, 1H) 8.19 (s, 1H), 8.15 (s, 1H), 7.99 (d,  $J = 8.85$  Hz, 1H), 7.82-7.76 (m, 1H), 7.59 (d,  $J = 8.85$  Hz, 1H), 7.32-7.24 (m, 2H), 4.08 (s, 3H), 4.04 (s, 3H), 3.89 (s, 3H) ppm;  $^{13}\text{C}$  NMR (125 MHz,  $\text{CDCl}_3 + \text{DMSO}-d_6$ ):  $\delta$  159.0, 153.1, 149.3, 148.9, 131.4, 130.5, 127.2, 126.4, 124.6, 124.3, 124.1, 122.1, 122.0, 116.4, 107.3, 104.1, 103.8, 55.7, 55.4, 55.1 ppm; HRMS (ESI):  $m/z$  calcd for  $\text{C}_{24}\text{H}_{19}\text{ClN}_2\text{O}_3$  419.1157, found 419.1150  $[\text{M} + \text{H}]^+$ .

4.1.5.15 *6-Fluoro-2-(3,6,7-trimethoxyphenanthren-9-yl)-1H-benzo[d]imidazole (10o)*.

Yellow solid, yield 75%; mp: 256–258 °C;  $^1\text{H}$  NMR (300 MHz,  $\text{DMSO}-d_6$ ):  $\delta$  8.50 (s, 1H)

8.01 (s, 1H), 7.89-7.78 (m, 4H), 7.48 (s, 1H), 7.23-7.20 (m, 1H), 7.07-7.00 (m, 1H), 4.13 (s, 3H), 4.05 (s, 3H), 3.97 (s, 3H) ppm;  $^{13}\text{C}$  NMR (125 MHz,  $\text{CDCl}_3$ +DMSO- $d_6$ ):  $\delta$  159.7, 158.4, 157.8, 152.9, 148.8, 148.3, 130.9, 130.0, 126.9, 124.1, 124.0, 122.2, 115.4, 115.0, 110.0, 109.7, 106.6, 102.8, 102.6, 100.5, 100.4, 55.3, 55.0, 54.8 ppm; HRMS (ESI):  $m/z$  calcd for  $\text{C}_{24}\text{H}_{19}\text{FN}_2\text{O}_3$  403.1452, found 403.1452  $[\text{M} + \text{H}]^+$ .

**4.1.5.16** *1-Benzyl-5-chloro-2-(3,6,7-trimethoxyphenanthren-9-yl)-1H-benzof[d]imidazole (10p)*.

White solid, yield 83%; mp: 201–203 °C;  $^1\text{H}$  NMR (500 MHz,  $\text{CDCl}_3$ ):  $\delta$  7.94-7.93 (m, 2H), 7.88 (d,  $J = 2.13$  Hz, 1H), 7.70 (s, 1H), 7.68 (d,  $J = 8.85$  Hz, 1H), 7.30-7.27 (m, 2H), 7.21-7.17 (m, 4H), 7.15 (s, 1H), 6.93-6.91 (m, 2H), 5.27 (s, 2H), 4.13 (s, 3H), 4.04 (s, 3H), 3.79 (s, 3H) ppm;  $^{13}\text{C}$  NMR (125 MHz,  $\text{CDCl}_3$ ):  $\delta$  152.1, 150.9, 150.0, 148.9, 148.8, 148.4, 140.0, 138.8, 134.0, 132.7, 131.2, 130.3, 127.4, 125.9, 124.8, 124.6, 124.2, 123.6, 123.3, 123.1, 108.6, 107.7, 105.2, 103.9, 103.7, 103.5, 55.9, 55.7, 55.4, 54.9 ppm; HRMS (ESI):  $m/z$  calcd for  $\text{C}_{31}\text{H}_{25}\text{ClN}_2\text{O}_3$  509.1626, found 509.1621  $[\text{M} + \text{H}]^+$ .

**4.1.5.17** *6-Bromo-2-(3,6,7-trimethoxyphenanthren-9-yl)-1H-imidazo[4,5-b]pyridine (10q)*.

Off white solid, yield 72%; mp: 206–208 °C;  $^1\text{H}$  NMR (500 MHz, DMSO- $d_6$ ):  $\delta$  8.78 (s, 1H), 8.47 (s, 1H), 8.29-8.15 (m, 4H), 7.99 (d,  $J = 8.85$  Hz, 1H), 7.33-7.30 (m, 1H), 4.08 (s, 3H), 4.05 (s, 3H), 3.89 (s, 3H) ppm;  $^{13}\text{C}$  NMR (125 MHz, DMSO- $d_6$ ):  $\delta$  150.3, 149.1, 148.9, 148.6, 126.8, 125.0, 124.9, 124.7, 124.2, 123.9, 122.5, 120.7, 118.2, 112.9, 110.9, 108.7, 107.3, 103.8, 103.5, 55.9, 55.8, 55.1 ppm; HRMS (ESI):  $m/z$  calcd for  $\text{C}_{23}\text{H}_{18}\text{BrN}_3\text{O}_3$  464.0604, found 464.0607  $[\text{M} + \text{H}]^+$ .

## 4.2 Biology

### 4.2.1. Cell Cultures

Cells were procured from National Centre for Cell Science (NCCS) Pune, India and stocks were maintained under sterile conditions. Breast (BT-549), triple negative breast (MDA-MB-453), prostate (PC-3 and DU145) and colon (HCT-116 and HCT-15) cancer cells were grown in tissue culture flasks in RPMI 1640 medium, Sigma, MEM (Minimum Essential Medium, Sigma) or DMEM (Dulbecco modified Eagle medium, Sigma) supplemented with 10% fetal bovine serum with 1X stabilized antibiotic-antimycotic solution (Sigma) in a  $\text{CO}_2$  incubator at 37 °C with 90% relative humidity and 5%  $\text{CO}_2$ .

### 4.2.2 MTT assay

MTT assay was performed to determine the anticancer activity for all the new compounds **10a-q**.  $1 \times 10^4$  cells per well were seeded in 100  $\mu\text{L}$  respective media, supplemented with 10% FBS in each well of 96-well microculture plates and incubated for 24 h, at 37 °C in a CO<sub>2</sub> incubator. Compounds, diluted to the required concentrations in culture medium, were added to the wells with respective vehicle control. After 48 h of incubation, 100  $\mu\text{L}$  MTT (3-(4,5-dimethylthiazol-2-yl)-2,5-diphenyl tetrazolium bromide) (5 mg/mL) was added to all the plates and incubated for 4 h. Then, the supernatant was carefully decanted from each well, formazon crystals were dissolved in 100  $\mu\text{L}$  of DMSO and absorbance at 570 nm wavelengths was recorded.

#### 4.2.3 Morphology studies using phase contrast microscopy

PC-3 cells were plated in 6 well culture plates with a density of  $1 \times 10^5$  cells/mL and allowed to adhere for overnight. Cells were incubated with different concentrations of **10o**. After 48 h, cells were observed for morphological changes and phase contrast microscope (Nikon) was used to capture the images.

#### 4.2.4 Acridine orange–ethidium bromide (AO–EB) staining

PC-3 cells were plated at a concentration of  $1 \times 10^6$  cell/ml and treated with increased concentration of compound **10o**. Plates were incubated at 37 °C in an atmosphere of 5% CO<sub>2</sub> for 48 h. 10  $\mu\text{L}$  of fluorescent dyes containing Acridine Orange (AO) and Ethidium Bromide (EB) added into each well in equal volumes (10  $\mu\text{g}/\text{mL}$ ) respectively and after 10 min the cells were visualized under fluorescence microscope (Nikon, Inc. Japan) with excitation (488 nm) and emission (550 nm) at 200x magnification.

#### 4.2.5 DAPI staining

DAPI staining was performed to observe alterations in Nuclear morphology. After treatment with **10o** for 48 h in PC-3 cells, cells were washed with PBS and solubilized with 0.1% Tween 20 for 10 min followed by staining with 1  $\mu\text{M}$  DAPI. Control and treated cells were observed with fluorescence microscope (Model: Nikon, Japan) with excitation at 359 nm and emission at 461 nm using DAPI filter at 200X magnification.

#### 4.2.6 Cell cycle analysis

The distribution of the cell population through different phases of cell cycle was analysed by Flow cytometric analysis (FACS). PC-3 cells were incubated with **10o** at different concentrations like 2.5  $\mu\text{M}$ , 5.0  $\mu\text{M}$ , and 10  $\mu\text{M}$  for 24 h. control and **10o** treated cells were

harvested, washed with PBS, fixed in 70% ethanol and stained with propidium iodide (50  $\mu\text{g}/\text{mL}$  sigma aldrich) in the presence of RNase A (20  $\mu\text{g}/\text{mL}$ ) containing 0.1% Triton X-100 for 30 min at 37°C in dark, and about 10000 events were analyzed by flow cytometer.

#### 4.2.7 Measurement of reactive oxygen species (ROS)

PC-3 cells were plated in 24 well plates at a density of ( $1 \times 10^6$  cells/mL) and allowed to adhere for overnight. Then the cells were treated with 2.5  $\mu\text{M}$ , 5.0  $\mu\text{M}$  and 10.0  $\mu\text{M}$  of active compound **10o** for 24 h. The media was replaced with culture medium containing DCFDA dye (10  $\mu\text{M}$ ) and incubated for 30 min dark. The fluorescence intensity from samples was analysed by spectrofluorometer at an excitation and emission wavelength of 488 and 525 nm, respectively.

#### 4.2.8 Analysis of mitochondrial membrane potential ( $D\Psi\text{m}$ )

PC-3 cells ( $1 \times 10^6$  cells/mL) were plated in 6 well plates and allowed to adhere for overnight. The cells were incubated with 2.5  $\mu\text{M}$ , 5.0  $\mu\text{M}$  and 10  $\mu\text{M}$  concentrations of the compound **10o** for 24 h. cells were collected, washed with PBS and resuspended in solution of JC-1 (2.5  $\mu\text{g}/\text{mL}$ ) and allowed for incubation at 310o C for 45 min. The cells were washed twice with PBS and cells were trypsinized, centrifuged and analyzed by flow cytometer (BD FACSVers<sup>TM</sup>, USA).

#### 4.2.9 Annexin V-FITC/Propidium iodide dual staining assay

The Annexin V-FITC/Propidium iodide dual staining assay was performed using PC-3 cells. To quantify the percentage of apoptotic cells, PC-3 cells ( $1 \times 10^6$  mL per well) were plated in six-well culture plates and allowed to grow for 24 h. after treatment with increasing concentrations of compound **10o** (2.5, 5.0 and 10  $\mu\text{M}$ ) for 24 h, cells were collected by trypsinisation. The collected cells were washed twice with ice-cold PBS, then incubated with 200  $\mu\text{L}$  x binding buffer containing 5  $\mu\text{L}$  Annexin V-FITC, and then in 300  $\mu\text{L}$  x binding buffer containing 5  $\mu\text{L}$  Propidium iodide (PI) for 5 min at room temp in the dark. After 15 min of incubation, cells were analyzed for apoptosis using flow-cytometer (BD FACSVers<sup>TM</sup>, USA).

#### 4.2.10 Relative Viscosity measurements

The viscosities of the complexes were determined by the Rolling-ball Viscometer, Lovis 2000 M/ME (Anton Paar GmbH, Graz, Austria), based on the falling ball principle. The temperature was controlled to  $\pm 0.005$  K by a built in Peltier thermostat. A calibrated glass

capillary (1.59 mm) with a steel ball was filled with the sample for measuring the ball falling time at angles in the range of 20° to 70°. The ball falling time and densities were used to estimate kinematic as well as dynamic viscosities at 25 °C. In each measurement, the uncertainty of the viscosity is 0.006 mPas. Titrations were performed for each derivative (5µM), while it was added to CT-DNA solution (50 µM). 5µM of Ethidium bromide, Doxorubicin and Hoechst 33258 solution was used as controls in the experiment. DNA solution was prepared in 100 mM Tris-HCl (pH 7.0). Data were presented as  $(\eta/\eta_0)^{1/3}$  versus the ratio of the concentration of the hybrid to CT-DNA, where  $\eta$  is the viscosity of CT-DNA in the presence of hybrid and  $\eta_0$  is the viscosity of CT-DNA alone.

#### 4.2.11 Molecular modelling studies

The title compounds were built using molecular builder of Maestro 10.4, prepared using Ligprep 3.6 and geometrically minimized with Macromodel 11.0 based on OPLS-2005 force field followed by conformational analysis. Truncated Newton Conjugate Gradient (TNCG) minimization method was used with 500 iterations and convergence threshold of 0.05 kJ/mol. The DNA duplex was prepared using protein preparation wizard. The Glide XP 6.9 algorithm was employed using a grid box volume of 10x 10x 10 Å.

#### Acknowledgements

N.P.K. and P.S are thankful to DoP, Ministry of Chemicals & Fertilizers, Govt. of India, New Delhi, for the award of NIPER fellowship. Dr. N. Shankaraiah thankful to SERB, DST, Govt. of India for the start-up grant (YSS-2015-001709).

#### 5. References

1. M. Rashid, A. Husain, R. Mishra, Eur. J. Med. Chem. 54 (2012) 855-866.
2. M.S. Ricci, W.-X. Zong, Oncologist. 11 (2006) 342-357.
3. G. Kibria, H. Hatakeyama, H. Harashima, Arch. Pharm. Res 37 (2014) 4-15; (b) A. Kamal, T.S. Reddy, S. Polepalli, S. Paidakula, V. Srinivasulu, V.G. Reddy, N. Jain, N. Shankaraiah, Bioorg. Med. Chem. Lett. 24 (2014) 3356-3360; (c) N.Shankaraiah, S. Nekkanti, K.J. Chudasama, K.R. Senwar, P. Sharma, M.K. Jeengar, V.G.M. Naidu, V.Srinivasulu, A. Kamal, Bioorg. Med. Chem. Lett. 24 (2014) 5413-5417; (d) A. Kamal, T.S. Reddy, S. Polepalli, N. Shalini, V.G. Reddy, A.V.S. Rao, N. Jain, N. Shankaraiah, Bioorg. Med. Chem. 22 (2014) 5466-5475.

4. (a) G.B. Jones, J.E. Mathews, *Tetrahedron Lett.* 53 (1997) 14599- 14614; (b) N. Shankaraiah, P. Sharma, S. Pedapati, S. Nekkanti, V. Srinivasulu, N.P. Kumar, A. Kamal, *Lett. Drug. Des. Disc.* 13 (2016) 335-342; (c) N. Shankaraiah, K.P.Siraj, S. Nekkanti, V. Srinivasulu, M. Satish, P. Sharma, K.R. Senwar, M.V.P.S. Vishnuvardhan, S. Ramakrishna, A. Kamal, *Bioorg. Chem.* 59 (2015) 130-139; (d) A. Kamal, K. Sreekanth, N. Shankaraiah, M. Satish, S. Nekkanti, V. Srinivasulu, *Bioorg. Chem* 59 (2015) 23-30.
5. (a) S.W. Fesik, *Nat. Rev. Cancer.* 5 (2005) 876-885 (b) N. Shankaraiah, N.P. Kumar, S.B. Amula, S. Nekkanti, M.K. Jeengar, V.G.M. Naidu, T.S. Reddy, A. Kamal, *Bioorg. Med. Chem. Lett.* 25 (2015) 4239-4244; (c) K.R. Senwar, P. Sharma, T.S. Reddy, D. Thummuri, V.G.M. Naidu, N. Shankaraiah, *Eur. J. Med. Chem.* 118 (2016) 34-46.
6. M. Deng, B. Su, H. Zhang, Y. Liu, Q. Wang, *RSC Advances.* 4 (2014) 14979-14984.
7. (a) L. Wei, A. Brossi, R. Kendall, K.F. Bastow, S.L. Morris-Natschke, Q. Shi, K.H. Lee, *Bioorg. Med. Chem.* 14 (2006) 6560-6569; (b) T. Ikeda, T. Yaegashi, T. Matsuzaki, R. Yamazaki, S. Hashimoto, S. Sawada, *Bioorg. Med. Chem. Lett.* 21 (2011) 5978-5981; (c) N.P. Kumar, P. Sharma, T.S. Reddy, S. Nekkanti, N. Shankaraiah, G. Lalitha, S.S. Kumari, S.K. Bhargava, V.G.M. Naidu, A. Kamal, *Eur. J. Med. Chem.* 127 (2017) 305-317; (d) N.P. Kumar, S. Nekkanti, S.S. Kumari, P. Sharma, N. Shankaraiah, *Bioorg. Med. Chem. Lett.* 27 (2017) 2369-2376.
8. M.G. Banwell, A. Bezos, C. Burns, I. Kruszelnicki, C.R. Parish, S. Su, M.O. Sydnes, *Bioorg. Med. Chem. Lett.* 16 (2006) 181-185.
9. J.Y. Choi, W. Gao, J. Odegard, H.S. Shiah, M. Kashgarian, J.M. McNiff, D.C. Baker, Y.C. Cheng, *J. Craft, Arthritis & Rheumatism.* 54 (2006) 3277-3283.
10. X. You, M. Pan, W. Gao, H. S. Shiah, J. Tao, D. Zhang, F. Koumpouras, S. Wang, H. Zhao, J.A. Madri, *Arthritis & Rheumatism.* 54 (2006) 877-886.
11. B. Baumgartner, C.A. Erdelmeier, A.D. Wright, T. Rali, O. Sticher, *Phytochemistry.* 29 (1990) 3327-3330.
12. H.M. Faidallah, K.A. Shaikh, T.R. Sobahi, K.A. Khan, A.M. Asiri, *Molecules,* 18 (2013) 15704-15716.
13. B. Su, C. Cai, M. Deng, D. Liang, L. Wang, Q. Wang, *Bioorg. Med. Chem. Lett.* 24 (2014) 2881-2884.
14. M. Wu, Z. W. Wang, Y.X. Liu, H.B. Song, A. Zhang, L.H. Meng, Q.M. Wang, *RSC Advances.* 37 (2013) 1817-1822.
15. Z. Xi, R. Zhang, Z. Yu, D. Quyang, R. Huang, *Bioorg. Med. Chem. Lett.* 15 (2005) 2673-2677.

16. (a) K.N. Rao, R.K. Bhattacharya, S.R. Venkatachalam, *Cancer Letters*. 128 (1998) 183-188; (b) X. Yang, Q. Shi, S.C. Yang, C.Y. Chen, S.L. Yu, K.F. Bastow, S.L.M. Natschke, P.C. Wu, C. Y. Lai, T.S. Wu, *J. Med. Chem.* 54 (2011) 5097-5107.
17. (a) Y. Bansal, O. Silakari, *Bioorg. Med. Chem. Lett.* 20 (2012) 6208-6236; (b) G. Yadav, S. Ganguly, *Eur. J. Med. Chem.* 97 (2015) 419-443; (c) Y. Tong, J.J. Bouska, P.A. Ellis, E. F. Johnson, J. Levenson, X. Liu, P.A. Marcotte, A.M. Oison, D.J. Osterling, M. Przytulinska, L.E. Rodriguez, Y. Shi, N. Soni, J. Stavropoulos, S. Thomas, C.K. Donawho, D.J. Frost, Y. Luo, V.L. Giranda, T.D. Penning, *J. Med. Chem.* 52 (2009) 6803-6813.
18. H. A. Barker, R.D. Smyth, H. Weisbacch, J.I. Toohey, J.N. Ladd, B. E. Volcanic, *J Biol Chem.* 235 (1960) 480-488.
19. I. Oren, O. Temiz, I. Yalcin, E. Sener, N. Altanlar, *Eur. J. Pharm. Sci.* 7 (1998) 153-160; (b) T. Hisano, M. Ichikawa, k. Tsumoto, M. Tasaki, *Chem. Pharm. Bull.* 30 (1982) 2996-3004.
20. (a) P. Sharma, T.S. Reddy, D. Thummuri, K.R. Senwar, N.P. Kumar, V.G.M. Naidu, S.K. Bhargava, N. Shankaraiah, *Eur. J. Med. Chem.* 124 (2016) 608-621; (b) A. Kamal, T.S. Reddy, M.V.P.S. Vishnuvardhan, V.K. Nimbarte, A.V.S. Rao, V. Srinivasulu, N. Shankaraiah, *Bioorg. Med. Chem.* 23 (2015) 4608-4623.
21. S.M. Sondhi, R. Rani, J. Singh, P. Roy, S.K. Agrawal, A.K. Saxena, *Bioorg. Med. Chem. Lett.* 20 (2010) 2306-2310.
22. H. Nakano, T. Inoue, N. Kawasaki, H. Miyataka, H. Matsumoto, T. Taguchi, N. Inagaki, H. Nagai, T. Satoh, *Bioorg. Med. Chem.* 8 (2000) 373-380.
23. M. Tuncbilek, H. Goker, R. Ertan, R. Eryigit, E. Kendi, N. Altanlar, *Arch. Pharm. Pharm. Med. Chem.* 330 (1997) 372-376.
24. Y. F. Li, G. F. Wang, P. L. He, W.G. Huang, F.H. Zhu, H.Y. Gao, W. Tang, Y. Luo, C. L. Feng, L.P. Shi, Y.D. Ren, W. Lu, J.P. Zuo, *J. Med. Chem.* 49 (2006) 4790-4794.
25. P. Chaudhuri, B. Ganguly, S. Bhattacharya, *J. Org. Chem.* 72 (2007) 1912-1923.
26. R. Abonia, J. Castillo, P. Cuervo, B. Insuasty, J. Quiroga, A. Ortiz, M. Nogueras, J. Cobo, *Eur. J. Org. Chem.* **2010**, 317-325.
27. A. Kamal, P. Praveen Kumar, M.N. Ahmed Khan, B.N. Sheshadri, O. Srinivas, *Lett. Drug. Des. Discov.* 12 (2015) 374-384.

28. M. Matsuyama, K. Funao, K. Kuratsukuri, T. Tanaka, Y. Kawahito, H. Sano, J. Chargui, J. L. Touraine, N. Yoshimura, R. Yoshimura, *Exp. Ther. Med.* 1 (2010) 301-306.
29. M. J. Niphakis, B.C. Gay, K.H. Hong, N.P. Bleeker, G.I. George, *Bioorg. Med. Chem.* 20 (2012) 5893-5900.
30. (a) P. Sharma, N.P. Kumar, N.H. Krishna, D. Prasanna, B. Sridhar, N. Shankaraiah, *Org. Chem. Front.* 3 (2016) 1503-1508; (b) S. Nekkanti, K. Veeramani, N.P. Kumar, N. Shankaraiah, *Green Chem.* 18 (2016) 3439-3447; (c) S. Nekkanti, N.P. Kumar, P. Sharma, A. Kamal, F.M. Nachtigall, O. Forero-Doria, L.S. Santos, N. Shankaraiah, *RSC Adv.* 6 (2016) 2671-2677.
31. (a) Y.Z. Lee, C.W. Yang, H.Y. Hsu, Y.Q. Qiu, T. K. Yeh, H.Y. Chang, Y.S. Chao, S.J. Lee, *J. Med. Chem.* 55 (2012) 10363-10377; (b) K. Wang, Y. Hu, M. Wu, Z. Li, Z. Liu, B. Su, A. Yu, Y. Liu, Q. Wang, *Tetrahedron.* 66 (2010) 9135-9140; (c) T.R. Govindachari, M. Lakshmikantham, K. Nagarajan, B. Pai, *Tetrahedron.* 4 (1958) 311-324; (d) H. Lv, J. Ren, S. Ma, S. Xu, J. Qu, Z. Liu, Q. Zhou, X. Chen, S. Yu, *PLoS ONE.* 7 (2012) e30342; (e) S. Kim, Y. M. Lee, J. Lee, T. Lee, Y. Fu, Y. Song, J. Cho, D. Kim, *J. Org. Chem.* 72 (2007) 4886-4891.
32. P. Sharma, K.R. Senwar, M. K. Jeengar, T.S. Reddy, V.G.M. Naidu, A. Kamal, N. Shankaraiah, *Eur. J. Med. Chem.* 104 (2015) 11-24.
33. K. Naumann, Bayer Crop Science, Brussels. 2003.
34. K.R. Senwar, P. Sharma, T.S. Reddy, M.K. Jeengar, V.L. Nayak, V.G.M. Naidu, A. Kamal, N. Shankaraiah, *Eur. J. Med. Chem.* 102 (2015) 413-424.
35. P. Sharma, D. Thummuri, T.S. Reddy, K.R. Senwar, V.G.M. Naidu, G. Srinivasulu, S.K. Bhargava, N. Shankaraiah, *Eur. J. Med. Chem.* 122 (2016) 584-600.
36. B.I. Tarnowski, F.G. Spinale, J.H. Nicholson, *Biotech Histochem.* 66 (1991) 297-302.
37. T.S. Reddy, V.G. Reddy, H. Kulhari, R. Shukla, A. Kamal, V. Bansal, *Eur. J. Med. Chem.* 117 (2016) 157-166.
38. E. Eruslanov, S. Kusmartsev, *Methods. Mol. Biol.* 594 (2010) 57-72.
39. N. Kulabas, E. Tatar, O.B. Ozakpinar, D. Ozsavci, C. Pannecouque, E.D. Clercq, I. Kucukguzel, *Eur. J. Med. Chem.* 121 (2016) 58-70.
40. C.P. Kumar, T.S. Reddy, P.S. Mainkar, V. Bansal, R. Shukla, S. Chandrasekhar, H.M. Hügel, *Eur. J. Med. Chem.* 108 (2016) 674-686.
41. N. Shankaraiah, C. Jadala, S. Nekkanti, K.R. Senwar, N. Nagesh, S. Shrivastava, V.G.M. Naidu, M. Satish, A. Kamal, *Bioorg. Chem.* 64 (2016) 42-50.

**Tables/Figures/Scheme captions**

**Table 1.** *In vitro* cytotoxic activity (IC<sub>50</sub> in  $\mu\text{M}$ )<sup>a</sup> of phenanthrene-9-benzimidazole conjugates **10a–q**

**Figure 1.** Structures of phenanthrene alkaloid, benzimidazole containing cytotoxic compounds and the designed phenanthrene-9 benzimidazole conjugates.

**Figure 2.** Phase contrast imaging: Effect of compound **10o** on the viability of PC-3 cells.

**Figure 3.** PC-3 cells were treated with various concentrations of the compound **10o** and stained with AO/EB. Apoptotic characteristics such as apoptotic bodies, membrane blebbing and dead cells were clearly observed.s

**Figure 4.** Nuclear morphology on PC-3 cells stained with DAPI. PC-3 cells treated with compound **10o** for 24 h were stained with DAPI. The images were captured with fluorescence microscope with a DAPI filter.ss

**Figure 5 (A and B).** Cell cycle analysis of PC-3 cancer cells treated with **10o** for 24 h. The cell cycle distribution was analysed by flow cytometry using propidium iodide staining method.

**Figure 6.** Effect of the compound **10o** on Reactive oxygen species (ROS) levels. Dose dependent increment of fluorescence was observed compared to control.

**Figure 7.** Effect of **10o** on the Mitochondrial membrane potential ( $\Delta\Psi\text{m}$ ). PC-3 cells were treated with 2.5  $\mu\text{M}$ , 5.0  $\mu\text{M}$  and 10.0  $\mu\text{M}$  of **10o**, incubated with JC-1 and analysed by flow cytometer (BD FACSVerse<sup>TM</sup>, USA).

**Figure 8.** Annexin binding assay for the detection of apoptosis. The compound **10o** treated cells were stained with Annexin V-FITC/PI and analysed for apoptosis. 10,000 cells from each sample were analysed by flowcytometry. The percentage of cells positive for Annexin

V-FITC and/or Propidium iodide is represented inside the quadrants. Cells in the upper left quadrant (Q1-UL; AV-/PI+): necrotic cells; lower left quadrant (Q1-LL; AV-/PI-): live cells; lower right quadrant (Q1-LR; AV+/PI-): early apoptotic cells and upper right quadrant (Q1-UR; AV+/PI +): late apoptotic cells.

**Figure 9.** Relative viscosity experiment of hybrids **10n** and **10o** with CT-DNA. Ethidium Bromide and Hoechst 33258 were used as controls. Data represents average from three individual experiments.

**Figure 10.** Side view (**A,C**) and top view (**B,D**) of the intercalation of **10n** (yellow) and **10o** (green), respectively between G–C base pairs of d(GAAGCTTC)<sub>2</sub>.

**Scheme 1.** Synthesis of different phenanthrene-9-benzimidazole conjugates **10a–q**.

## Tables/Figures/Schemes

**Table 1.** *In vitro* cytotoxic activity (IC<sub>50</sub> in μM)<sup>a</sup> of phenanthrene-9-benzimidazole conjugates **10a–q**

Compound	BT-549 <sup>b</sup>	MDA-MB-453 <sup>c</sup>	HCT-116 <sup>d</sup>	PC-3 <sup>e</sup>	DU145 <sup>f</sup>	HCT-15 <sup>g</sup>
<b>10a</b>	>20	>20	>20	12.8±0.24	18.9±0.81	>20
<b>10b</b>	>20	15.1±0.16	>20	15.7±0.11	>20	>20
<b>10c</b>	>20	9.42±0.14	>20	18.9±0.31	>20	>20
<b>10d</b>	10.8±0.06	>20	>20	14.6±0.19	>20	9.42±0.21
<b>10e</b>	>20	10.6±0.32	9.92±0.82	10.2±0.25	12.7±0.19	8.34±0.15
<b>10f</b>	>20	>20	>20	16.7±0.72	17.2±0.42	>20
<b>10g</b>	11.5±0.41	9.98±0.95	8.91±0.72	13.1±0.42	>20	10.15±0.2
<b>10h</b>	>20	>20	>20	>20	8.21±0.5	>20
<b>10i</b>	7.15±0.9	>20	>20	18.3±0.51	>20	>20
<b>10j</b>	>20	>20	>20	>20	10±0.35	>20
<b>10k</b>	>20	17.3±0.31	>20	11.5±0.17	>20	10.31±0.4
<b>10l</b>	>20	16.5±0.15	>20	12.8±0.08	>20	15.6±0.16
<b>10m</b>	11.4±0.35	>20	>20	>20	17.2±0.42	>20
<b>10n</b>	14.2±0.26	>20	11.3±0.46	7.24±0.98	>20	>20
<b>10o</b>	13.2±0.24	6.61±0.9	>20	6.32±0.09	>20	>20
<b>10p</b>	>20	7.20±0.18	>20	>20	>20	14.1±0.61
<b>10q</b>	7.91±0.23	>20	>20	11.3±0.46	>20	>20
<b>Nocodazole<sup>h</sup></b>	-	0.91±0.07	1.06±0.21	1.84±0.1	1.14±0.05	-
<b>5-FU<sup>i</sup></b>	-	-	8.62±0.87	1.2±0.01	2.18±0.33	-
<b>Doxorubicin<sup>j</sup></b>	-	1.99±1.75	1.01±0.09	0.19±0.01	1.91±0.13	-

<sup>a</sup>50% inhibitory concentration after 48 h of compound treatment; <sup>b</sup>Breast cancer cells; <sup>c</sup>triple negative breast cancer cells; <sup>d,g</sup>Colon cancer cells; <sup>e,f</sup>prostate cancer cells; <sup>h</sup>nocodazole, <sup>i</sup>5-fluorouracil: positive control, <sup>j</sup>doxorubicin: standard drug.

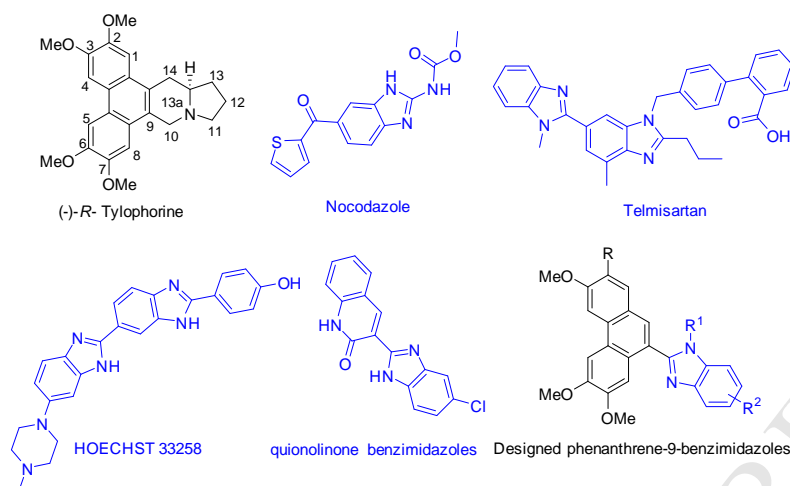


**Figure 1.** Structures of phenanthrene alkaloid, benzimidazole containing cytotoxic compounds and the designed phenanthrene-9 benzimidazole conjugates.

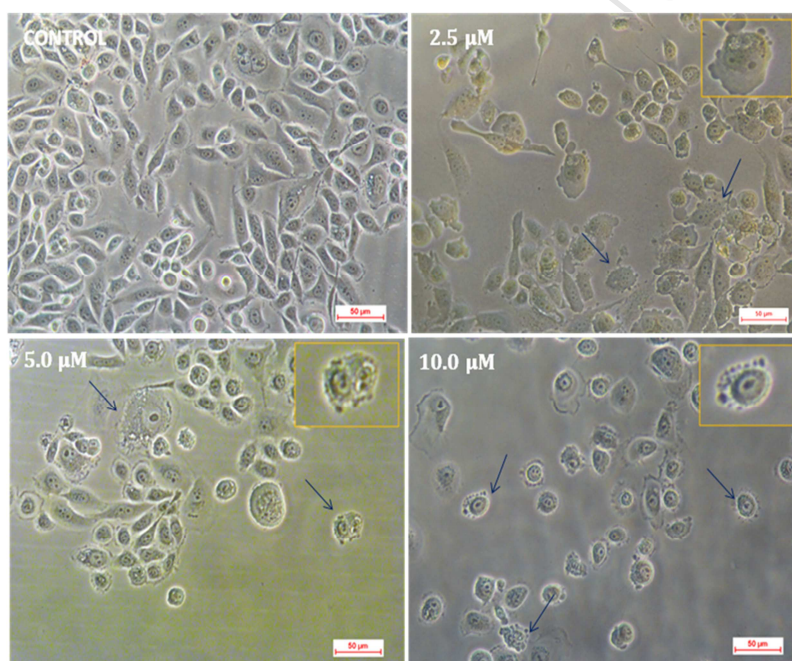


**Figure 2.** Phase contrast imaging: Effect of compound **10o** on the viability of PC-3 cells.

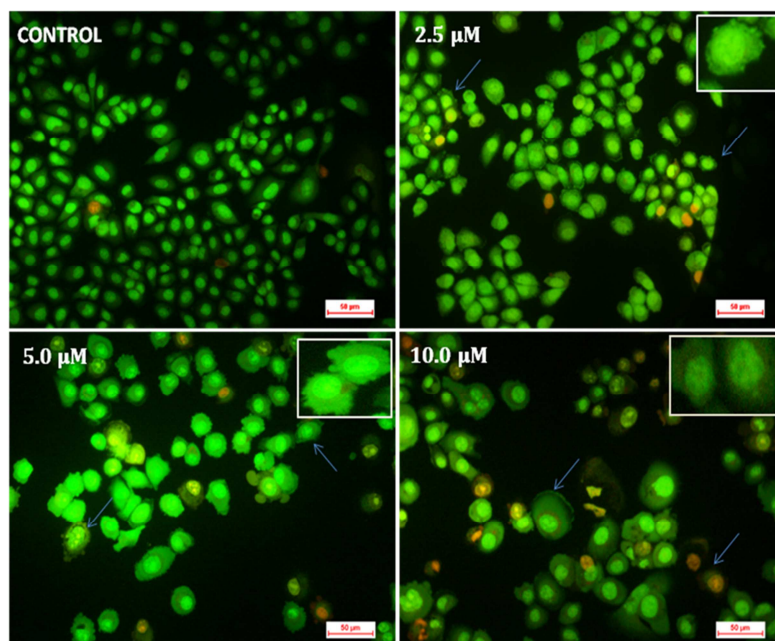


**Figure 3.** PC-3 cells were treated with various concentrations of the compound **10o** and stained with AO/EB. Apoptotic characteristics such as apoptotic bodies, membrane blebbing and dead cells were clearly observed.

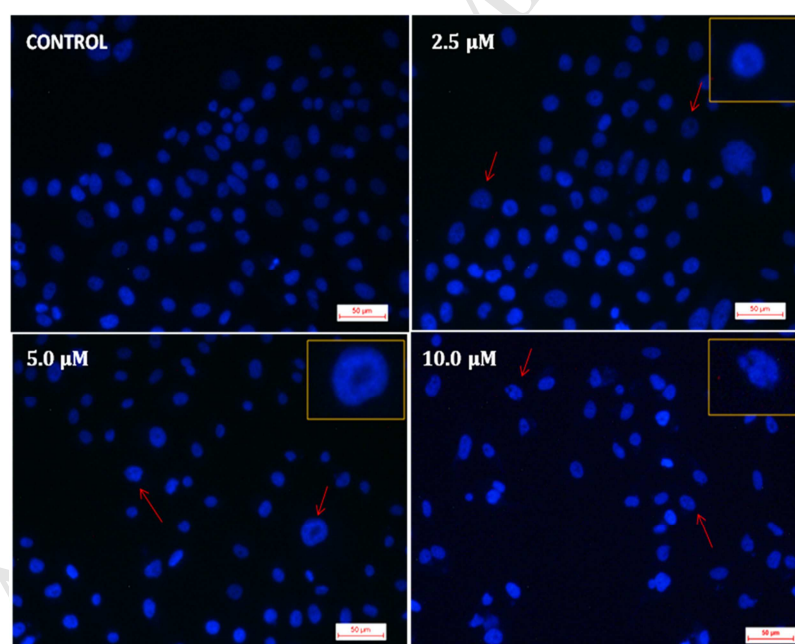
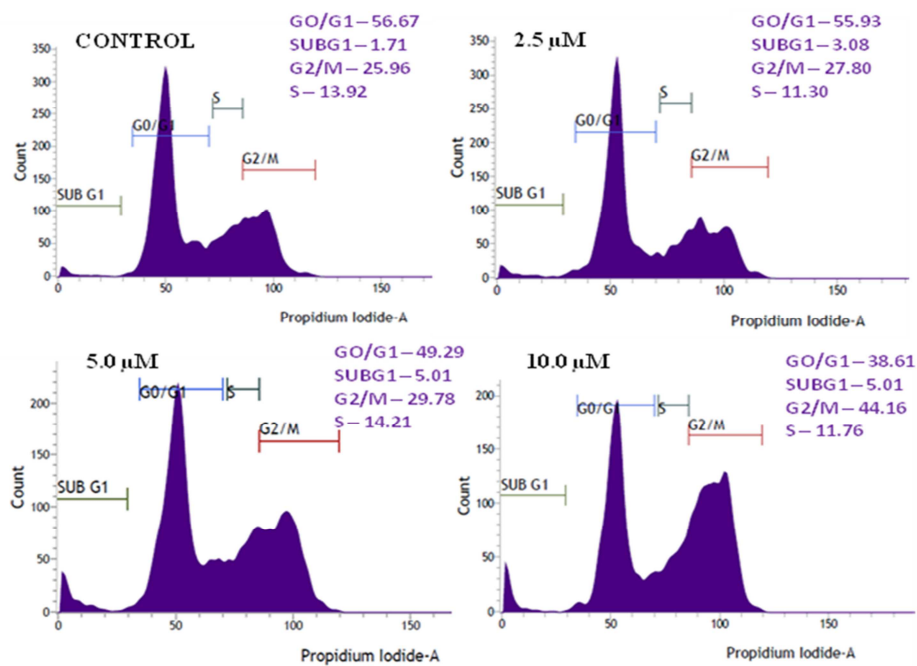
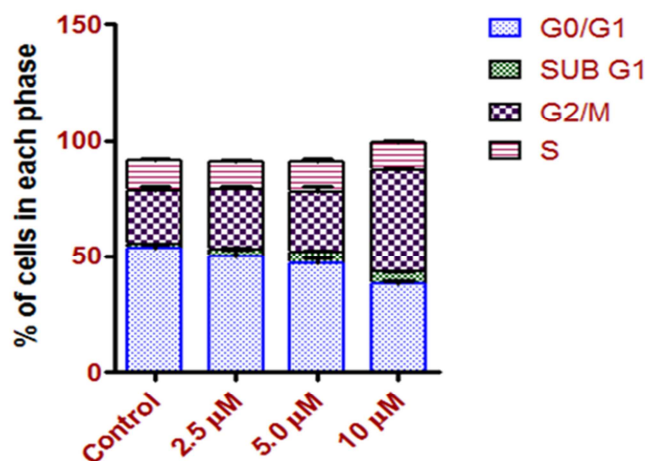


**Figure 4.** Nuclear morphology on PC-3 cells stained with DAPI. PC-3 cells treated with compound **10o** for 24 h were stained with DAPI. The images were captured with fluorescence microscope with a DAPI filter.

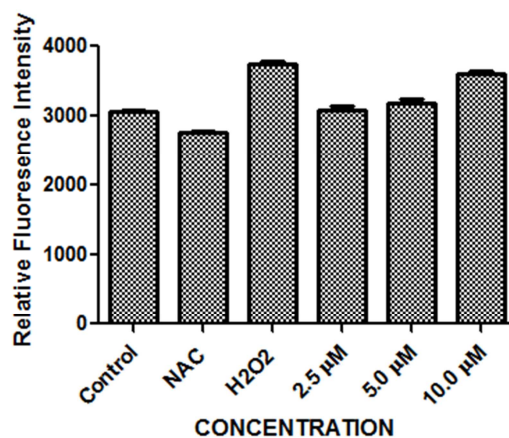


A

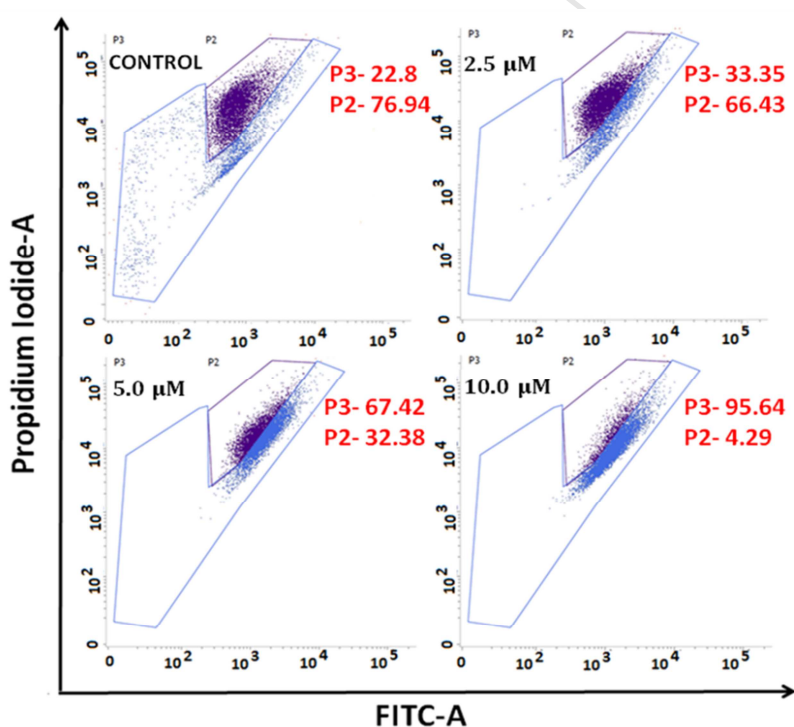


B

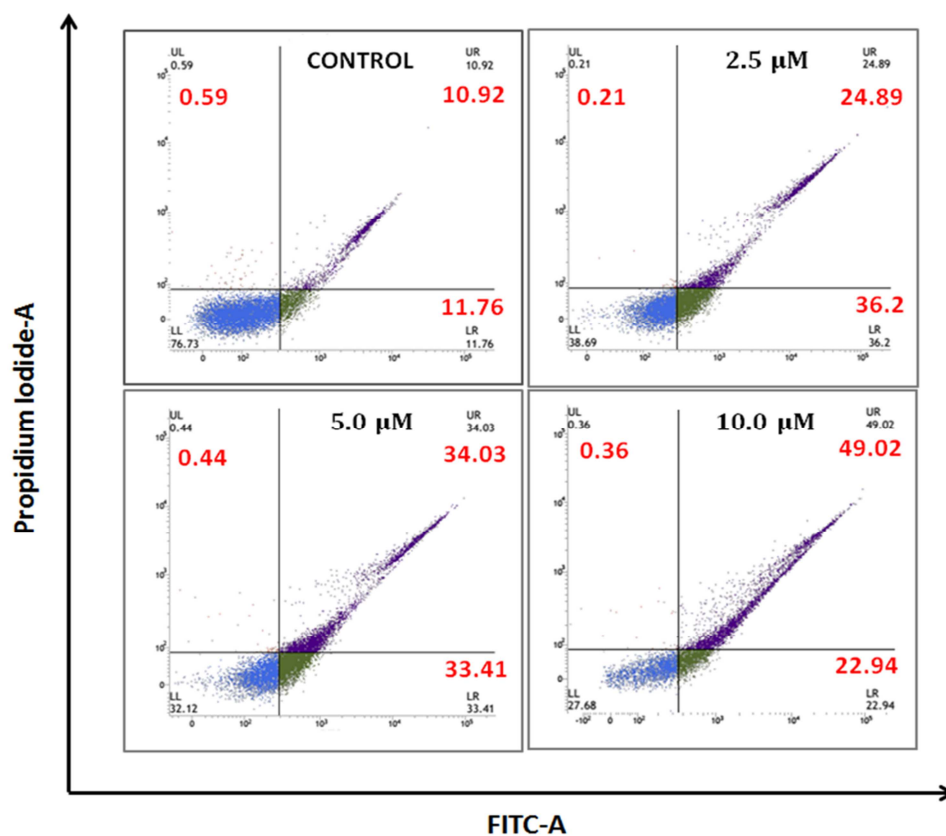
**Figure 5 (A and B).** Cell cycle analysis of PC-3 cancer cells treated with **10o** for 24 h. The cell cycle distribution was analysed by flow cytometry using propidium iodide staining method.



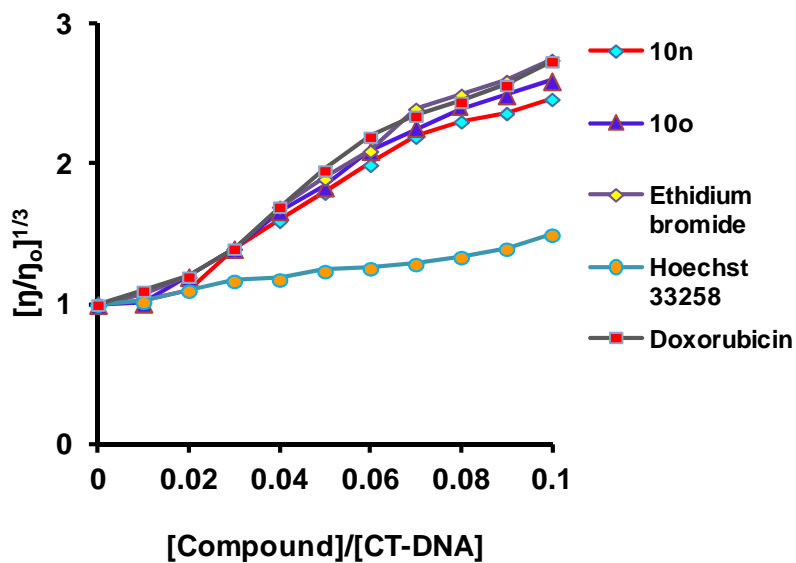
**Figure 6.** Effect of the compound **10o** on Reactive oxygen species (ROS) levels. Dose dependent increment of fluorescence was observed compared to control.



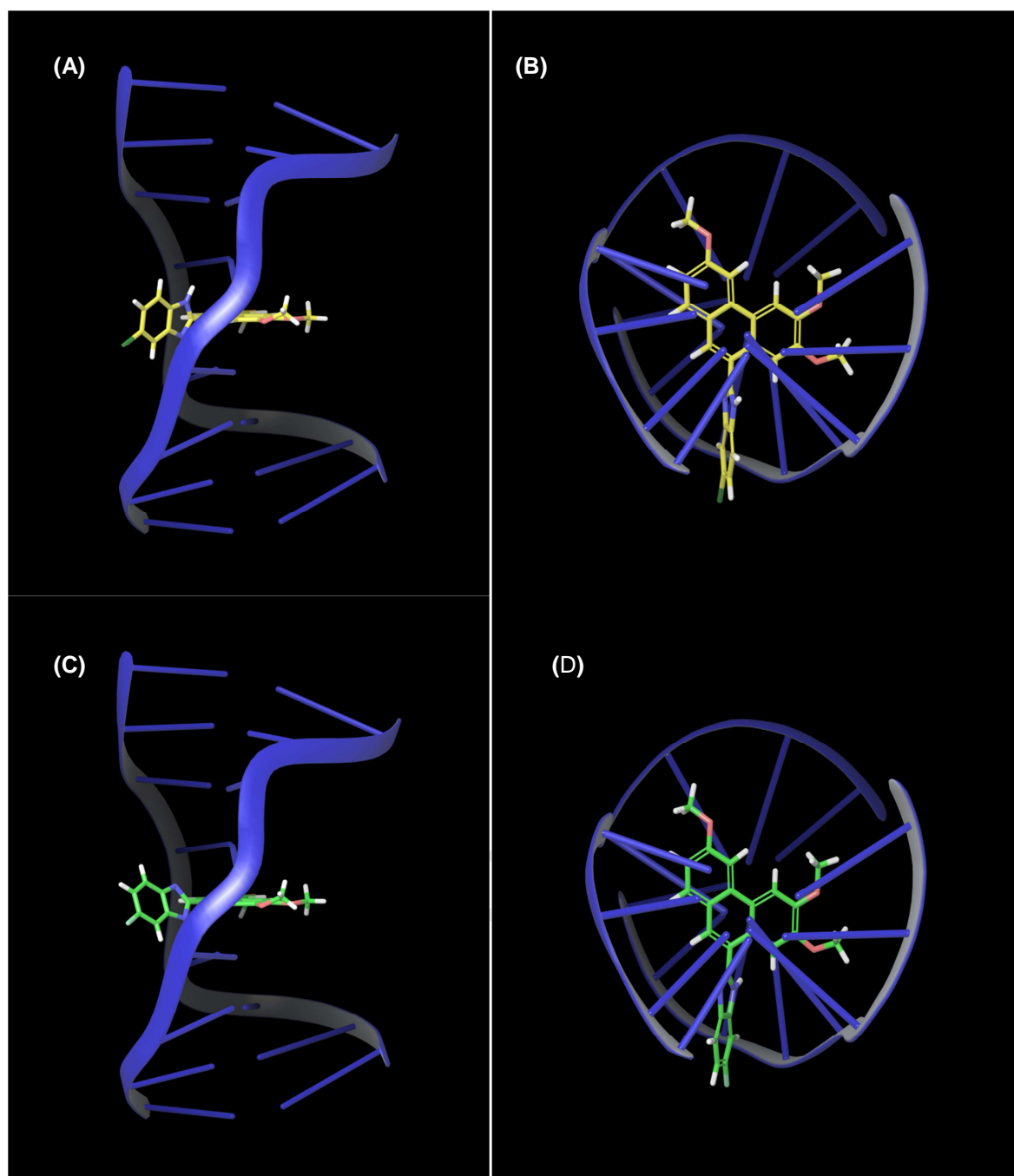
**Figure 7.** Effect of **10o** on the Mitochondrial membrane potential ( $\Delta\Psi_m$ ). PC-3 cells were treated with 2.5  $\mu$ M, 5.0  $\mu$ M and 10.0  $\mu$ M of **10o**, incubated with JC-1 and analysed by flow cytometer (BD FACSVerse<sup>TM</sup>, USA).



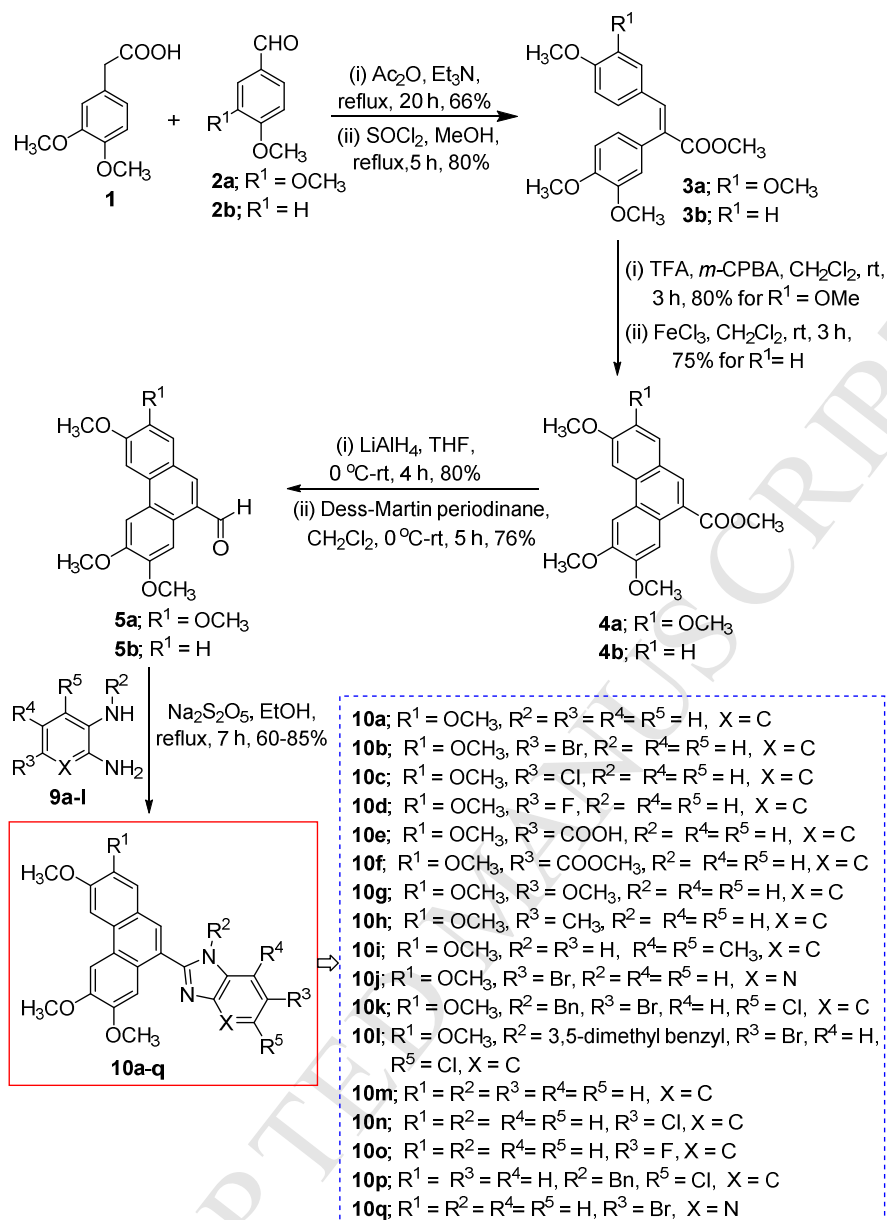
**Figure 8.** Annexin binding assay for the detection of apoptosis. The compound **10o** treated cells were stained with Annexin V-FITC/PI and analysed for apoptosis. 10,000 cells from each sample were analysed by flowcytometry. The percentage of cells positive for Annexin V-FITC and/or Propidium iodide is represented inside the quadrants. Cells in the upper left quadrant (Q1-UL; AV-/PI+): necrotic cells; lower left quadrant (Q1-LL; AV-/PI-): live cells; lower right quadrant (Q1-LR; AV+/PI-): early apoptotic cells and upper right quadrant (Q1-UR; AV+/PI +): late apoptotic cells.

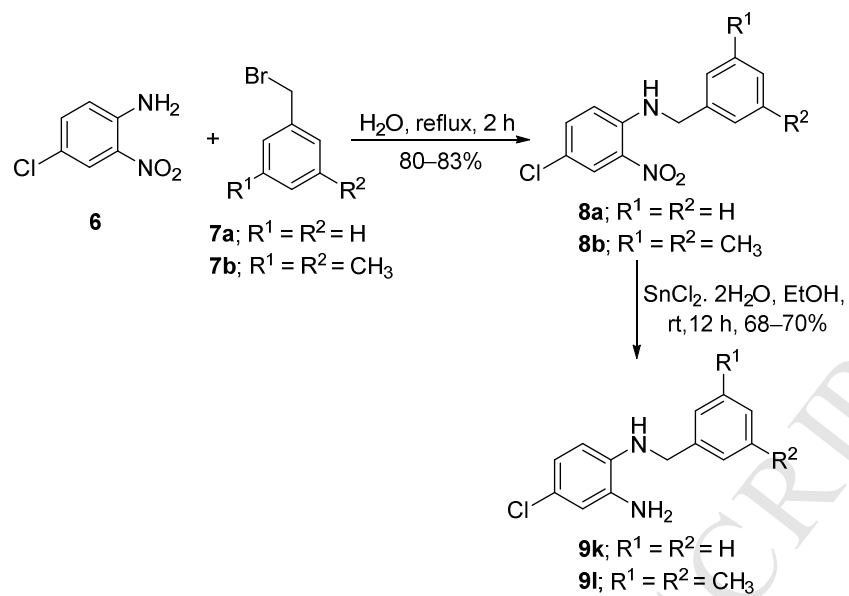


**Figure 9.** Relative viscosity experiment of hybrids **10n** and **10o** with CT-DNA. Ethidium Bromide, Doxorubicin and Hoechst 33258 were used as controls. Data represents average from three individual experiments.



**Figure 10.** Side view (A,C) and top view (B,D) of the intercalation of **10n** (yellow) and **10o** (green), respectively between G–C base pairs of d(GAAGCTTC)<sub>2</sub>.

Scheme 1. Synthesis of different phenanthrene-9-benzimidazole conjugates **10a–q**.



**Scheme 2.** Synthesis of *N*-benzylated *o*-phenylene diamines **9k,l**.

**Research Highlights**

- A new series of phenanthren-9-benzimidazoles has been synthesized.
- Cytotoxicity on selected cancer cell lines and apoptosis inducing studies.
- Test compound **10o** induced G2/M cell cycle arrest in PC-3 cells.
- **10o** enhanced ROS generation and caused the collapse of  $D\Psi m$ .
- DNA intercalation supported by relative viscosity studies and molecular docking.